Chapter 1 ►

Fundamentals of Poromechanics

Yves Guéguen[1]
Luc Dormieux[2]
Maurice Boutéca[3]

1.1 Introduction

The mechanical behavior of the Earth's crust is often modeled as that of a porous, fluid-saturated medium. Crustal rocks, as are many other solids, are porous and fluid saturated down to at least 10 km depth. Because they are made of minerals and open pores, they show an internal structure. Classical continuum mechanics describe such a medium as an idealized continuum model where all defined mechanical quantities are averaged over spatial and temporal scales that are large compared with those of the microscale process, but small compared with those of the investigated phenomenon. We follow this type of approach in this chapter's presentation of the classical macroscopic theories of porous rock deformation. Such a separation of scales is a necessary condition for developing a macroscopic formulation.

A complementary point of view is that of mixture theory. In that approach, solids with empty pore spaces can be treated relatively easily because all the components have the same motion when the solid is deformed. However, if the porous solid is filled with liquid, the solid and liquid constituents have different motion, and so the description of the mechanical behavior is more difficult. Interactions are taking place between the constituents. A convenient way to approximately solve that problem is to idealize the saturated rock as a mixture of two components that would fill the total space shaped by the porous solid. This is the model of mixture theory where each component occupies the total volume of space simultaneously

[1]Ecole Normale Supérieure, ENS, 24 rue Lhomond, 75231 Paris Cedex 05, France. yves.gueguen@ens.fr

[2]CERMMO, ENPC, 6-8 Avenue Blaise Pascal, Champs sur Marne, 77455, Marne la Vallée Cedex 2, France. dormieux@cermmo-omp.enpc.fr

[3]Institut Français du Pétrole, 1 et 4 avenue de Bois-Preau, 92852 Rueil-Malmaison Cedex, France. cepm@francenet.fr

with the others. The assumptions of the theory of mixtures are not completely valid for fluid-saturated rocks, because the solid and fluid phases are not miscible phases. This theory yields, however, a possible framework for the macroscopic treatment of liquid-saturated porous solids. An additional assumption is that only the fluid phase is allowed to leave the total space defined by the porous body. The pores are assumed to be statistically distributed and the porosity value fixes the ratio of the pore volume to the total porous body volume. Introducing the above assumptions means that the microscale should be taken into consideration. For that reason, the microscopic approach is developed in this chapter along with the classical macroscopic theory. Although this is unusual, we believe that it gives a better insight into rock behavior.

This chapter examines the most important mechanical types of behavior that can be observed for porous crustal rocks: small reversible deformation (poroelasticity), large irreversible deformation (poroplasticity), and rupture. Some complementary results on each of these are given in other chapters when appropriate. Dynamic effects are clearly out of the scope of this book, which focuses on quasi-static behavior.

1.2 Poroelasticity

Poroelasticity theory accounts reasonably well for small deformations of a fluid-saturated porous solid. It is an extension of elasticity theory to the precise situation we are interested in: that of a porous rock submitted to a small reversible strain. Reversibility is a major assumption because it allows us to develop the theory within the framework of classical thermodynamics. The extension to the theory of elastic behavior of a solid medium is that the fluid phase is taken into account, and this implies that two additional parameters are required to describe the thermodynamic state of the fluid: its pressure and its volume (or mass). Two possible descriptions are very useful:t he drained description, where the fluid pressure is the appropriate thermodynamic variable, and the undrained description, where the mass content is the appropriate thermodynamic variable. The fluid is viscous and compressible. The isothermal theory of poroelasticity was first presented by Biot (1941, 1955, 1956, 1957, 1972), and later reformulated by Rice and Cleary (1976) and Coussy (1991). Nonisothermal effects were later considered by Palciauskas and Domenico (1982) and McTigue (1986). Nonlinear poroelasticity was introduced by Biot (1973). Different reviews of poroelastic theory have been published by Detournay and Cheng (1993), Zimmerman (2000), Rudnicki (2002). Wang (2000) has presented a monograph on the theory of linear poroelasticity with applications to geomechanics and hydrogeology.

1.2.1 Linear Isothermal Poroelasticity

We follow here the classical sign convention of elasticity: compressive stresses are considered to be negative for the solid rock but fluid pressure is positive. We

consider the linear quasi-static isothermal theory, and assume that the rock at a macroscopic scale can be viewed as isotropic and homogeneous. Let P be the mean pressure, $P = -1/3\sigma_{kk}$, where σ_{ij} is a component of the stress tensor, defined as the measure of total force per unit area of an element of porous rock. Let p be the fluid pore pressure, which is the equilibrium fluid pressure inside the connected and saturated pores: p can be understood as the pressure on an imagined fluid reservoir that would equilibrate an element of rock to which it is connected from either giving off or receiving fluid from the reservoir. We assume that all pores are connected. In addition, let m be the fluid mass content per unit volume in the reference state. Fluid mass density ρ is defined locally as the mass density of fluid in the equilibrating reservoir. The apparent fluid volume fraction is $v = m/\rho$. Because we are considering a saturated rock, $v_0 = \Phi_0$, where Φ_0 is the initial porosity of a given porous rock volume V_0. In the deformed state, however, the volume V_0 is transformed into V so that $v - v_0$ is not identical to $\Phi - \Phi_0$ because $\Phi = V_p/V$, where V_p is the pore volume in the rock volume V: $v = V_p/V_0 = \Phi(V/V_0)$. In general the fluid is compressible and its density depends on p: $\rho = \rho(p)$. Only isothermal deformations are considered in this section. Linear poroelasticity is not restricted to fluids of low compressibility. The drained description is convenient to deal with highly compressible fluids. Two types of deformation will be considered: *drained* deformation refers to deformations at constant fluid pore pressure p, *undrained* deformation refers to deformations at constant fluid mass content m. Strain refers to the relative displacement of solid points in the solid phase. The components of the strain tensor are $\epsilon_{ij} = 1/2(\partial_j u_i + \partial_i u_j)$, where u_i is the displacement vector component. Stress, strain, and fluid pressure will be defined as small perturbations with respect to a given equilibrium state, so that body forces are ignored. The rock has an apparent elastic bulk modulus for drained conditions K

$$\frac{1}{K} = -\frac{1}{V}\left(\frac{\partial V}{\partial P}\right)_p. \tag{1.1}$$

Effective Stress Concept

The concept of effective stress is of great importance to poroelasticity. As an introductory step, let us consider first the case of effective pressure. The effective pressure P_e is defined by

$$P_e = P - bp, \tag{1.2}$$

where b is the Biot coefficient, which will be computed as follows. The elastic deformation of a rock sample submitted to both an isotropic pressure P and a pore pressure p can be obtained by superimposing two states of equilibrium (Figure 1.1). The first one corresponds to a pressure $P - p$ applied to the external surface of the rock and a zero fluid pressure within the pores. The second one is that of the same rock sample submitted to a pressure p on both the external surface of the rock

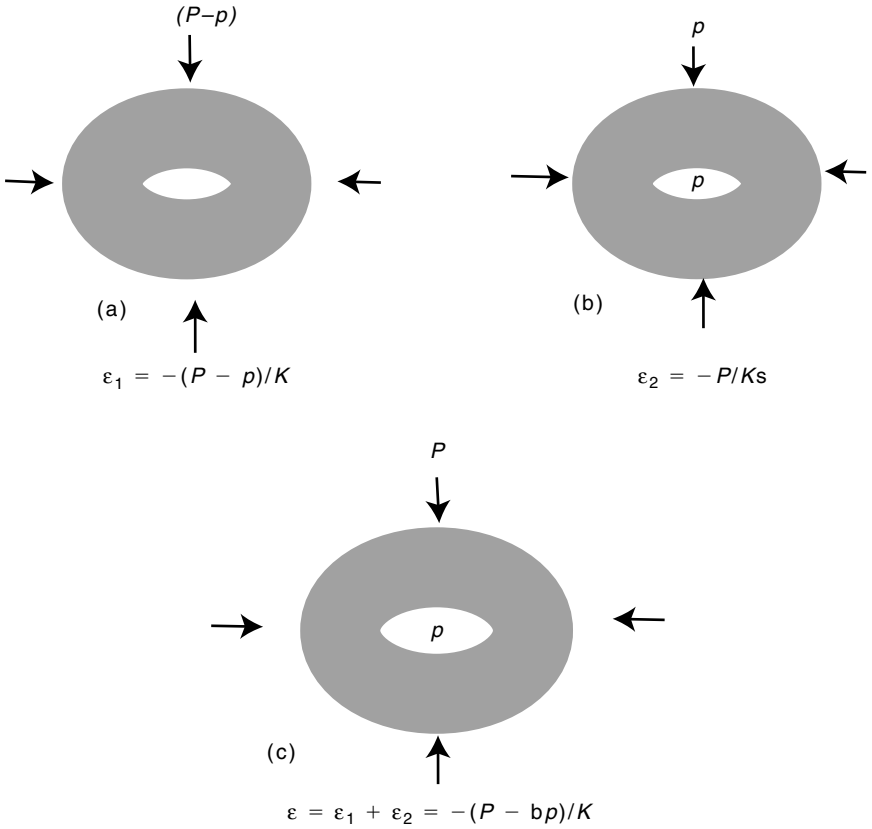

Figure 1.1 ► A porous rock submitted to an isotropic pressure P on its external surface and a pore pressure p (c). This stress state is obtained by superimposing (a) a pressure $(P-p)$ on the external surface and a zero pressure in the pores and (b) a pressure p on the external surface and in the pores.

and the internal surfaces of the pores. In this last case, the pores can be ignored for the overall rock deformation because they are at the same pressure as the solid phase. The rock, including the pores, is in a homogeneous isotropic stress state and "looks" as if it had no pores. Let us then introduce K_s, the bulk modulus of the solid phase. Because we assumed that the rock is homogeneous, that all pores are connected, and that the solid and fluid phases are chemically inert, a single modulus K_s is sufficient to account for the solid-phase behavior. The modulus K_s is defined by

$$\frac{1}{K_s} = -\frac{1}{V}\left(\frac{\partial V}{\partial p}\right)_{(P-p)}. \tag{1.3}$$

Because of the above assumptions, this modulus is identical to another modulus noted sometimes as K''_s or K_Φ and defined as

$$\frac{1}{K''_s} = -\frac{1}{V_p}\left(\frac{\partial V_p}{\partial p}\right)_{(P-p)}. \tag{1.4}$$

The elastic volumic strain ϵ_{kk} is noted ε. Its value in this second case is

$$\varepsilon_2 = -\frac{p}{K_s}, \tag{1.5}$$

whereas in the first case

$$\varepsilon_1 = -\frac{P-p}{K}. \tag{1.6}$$

Because of the linearity, we can superimpose both strains to get the overall volumic strain of the rock submitted to both an isotropic pressure P and a pore pressure p:

$$\varepsilon = -\frac{P-p}{K} - \frac{p}{K_s} = -\frac{1}{K}(P - bp), \tag{1.7}$$

where the Biot coefficient is found to be

$$b = \left(\frac{\partial P}{\partial p}\right)_\varepsilon = 1 - \frac{K}{K_s}. \tag{1.8}$$

Since $K \leq K_s$, the Biot parameter is a nondimensional parameter such that $b \leq 1$. The volumic strain is that which would be observed in a nonporous rock of bulk modulus K submitted to effective pressure $P_e = P - bp$. Effective stresses are defined by a straightforward extension of the above relation

$$(\sigma_{ij})^{eff} = \sigma_{ij} + bp\delta_{ij}. \tag{1.9}$$

Only normal stresses are involved because shear stresses (off diagonal stresses) remain unaffected by the pore pressure. For soft material, $K \ll K_s$, and the Terzaghi effective stress is recovered since $b = 1$ (von Terzaghi and Frölich, 1936).

Micromechanical Approach to Poroelastic Behavior

The reader not familiar with the micro–macro averaging techniques and/or not interested in the microscopic approach may skip this section. Some insight into the previous results can be gained from looking at porous rock starting from a microscopic description and relating macroscopic quantities to microscopic ones. This type of approach has been followed by some authors by assuming specific pore geometrical shapes (Zimmerman, 1991; Zimmerman 2000). Using such assumptions make it possible to derive macroscopic poroelastic parameters from the

values of the constituents' properties (i.e., elastic moduli of the solid and fluid phases, porosity, aspect ratios of pores). Effective medium theory (EMT) is an efficient tool for this type of calculation. Let us investigate, without any specific geometrical assumption, how to take advantage of this complementary point of view. The micromechanical approach relies on the assumption that there exists a representative elementary volume (REV) Ω (Figure 1.2). At the macroscopic scale, the latter is an infinitesimal part of a macroscopic structure. Its characteristic size is therefore small with respect to that of the structure. From a macroscopic point of view, the REV appears as the superposition of a solid skeleton particle and of a fluid particle, both located at the same macroscopic point. At each point, we have defined the macroscopic quantities u_i, displacement vector components, ϵ_{ij}, strain tensor components, and σ_{ij}, stress tensor components. In contrast, the microscopic scale reveals the geometry of the microstructure. At the microscopic scale, the solid and the fluid phases in the REV appear as two geometrically distinct domains. This means that the position vector of a material point lies either in the fluid phase or in the solid phase. As for the experimental approach, the micromechanical one aims at determining the macroscopic behavior. However, instead of applying the loading to a sample in a laboratory experiment, the micromechanical approach defines a boundary value problem on the REV considered as a mechanical structure, the latter playing the role of the sample in a theoretical experiment. Then, if the mechanical behavior of the constituents is known, the macroscopic behavior can be theoretically determined from the solution of this boundary value problem. Let u_i^s, e_{ij} , and s_{ij} respectively denote the displacement vector, strain tensor, and stress tensor components induced in the solid phase by the mechanical loading applied to the REV. Exactly as for a sample in a laboratory experiment, the size of the REV must be large with respect to that of the heterogeneities (solid grain or pore). This is a required condition to get a representative response of the

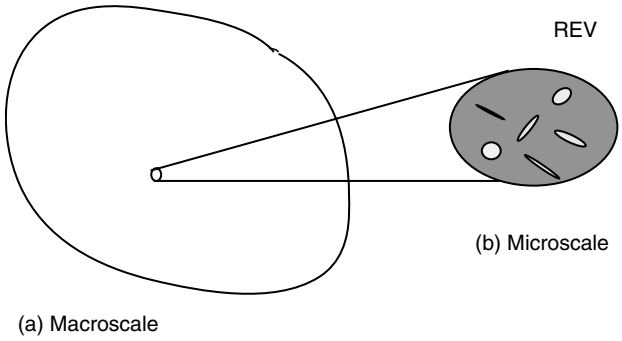

Figure 1.2 ► Representative elementary volume (REV). Macroscopic description—any point of the porous rock corresponds to an average over an REV centered on this point (a). Microscopic description—within the REV, the microstructure can be described, showing pores, cracks, etc. (b).

REV. The application of this methodology first requires defining how the boundary conditions on the REV are related to the macroscopic quantities, namely, the stress tensor σ_{ij}, strain tensor ϵ_{ij}, and the pore pressure p. We consider in the following the general case of an anisotropic rock.

We adopt a nonsymmetric point of view that considers the REV as an open system that always comprises the same solid material, while exchanging fluid mass through its boundary. We shall define at any time the location of the boundary of the REV as a function of the macroscopic strain tensor ϵ_{ij}. The macroscopic fluid and skeleton particles will then correspond to the fluid and solid materials within this closed boundary. As stated before, the skeleton particle, although subjected to strain, will remain constituted of the same solid. In contrast, the mass of the macroscopic fluid particle will be a function of time. In addition, to be able to determine the location of the fluid–solid interface inside the REV, we shall define a micromechanical problem on the boundary of the solid part of the REV. The solution of the latter will provide us at any time with the boundaries of both the solid and fluid domains.

Let us consider the REV in its reference state, in which it occupies the volume Ω^0. Its boundary $\partial\Omega^0$ comprises the solid–solid interface S^0_{ss} as well as the fluid–fluid interface S^0_{ff}. Now, let Ω denote the volume occupied by the REV at time t. The boundary $\partial\Omega$ is defined as the image of $\partial\Omega^0$ by a homogeneous transformation associated with the strain tensor ϵ_{ij}:

$$\begin{array}{ll} S^0_{ff}: & u_i = \epsilon_{ij} x_j \qquad (a) \\ S^0_{ss}: & u_i = \epsilon_{ij} x_j \qquad (b) \end{array} \tag{1.10}$$

This condition holds on S^0_{ff} as well as on S^0_{ss}. However, as we shall see, its physical meaning is not the same on the two parts of $\partial\Omega^0$.

The solid–fluid interface S_{sf} is subjected to the pressure p existing in the fluid:

$$S_{sf}: s_{ij} n_j = -p\, n_i \tag{1.11}$$

The local momentum balance equation in both the solid and fluid domains is

$$s_{ij,j} = 0 \tag{1.12}$$

The case of a nonlinear elastic solid material has been considered by De Buhan et al. (1998) and Dormieux et al. (2002). For simplicity, it is assumed here that the solid phase has a linear elastic behavior, characterized in the general anisotropic case by the elastic moduli C^s_{ijkl}:

$$s_{ij} = C^s_{ijkl} e_{lk}. \tag{1.13}$$

Equations (1.12) and (1.13), together with (1.10b) and (1.11), define a well-posed micromechanical problem on the solid domain Ω^0_s.

At any time, the total macroscopic stress σ_{ij} is defined as the average of the microscopic stress $< s_{ij} >$:

$$\sigma_{ij} = < s_{ij} > = \frac{1}{\Omega} \int_{\Omega} s_{ij} \, d\Omega. \tag{1.14}$$

From the local momentum balance equation (1.12), one obtains the identity $(x_k s_{ij})_{,j} = s_{ik}$. Integration of the latter over Ω^0 reveals that the macroscopic stress can be alternatively derived from the value of the microscopic stress on the REV boundary:

$$\sigma_{ij} = < s_{ij} > = \frac{1}{\mid \Omega^0 \mid} \int_{\Omega^0} (\chi_j s_{ij})_{,l} \, d\Omega = \frac{1}{\mid \Omega^0 \mid} \int_{\partial\Omega^0} \chi_j s_{ij} n_l \, dS. \tag{1.15}$$

The microscopic stress is uniform within the fluid phase, where we have

$$s_{ij} = -p \, \delta_{ij}. \tag{1.16}$$

Hence, the macroscopic total stress tensor σ_{ij} is

$$\sigma_{ij} = (1 - \Phi)\sigma^s_{ij} - \Phi p \delta_{ij}, \tag{1.17}$$

where σ^s_{ij} denotes the average of the microscopic stress field over the solid domain:

$$\sigma^s_{ij} = \frac{1}{\Omega_s} \int_{\Omega_s} s_{ij} \, d\Omega. \tag{1.18}$$

Because of the linearity of the micromechanical problem in equations (1.10b) through (1.13), the solution, i.e., the microscopic stress field s_{ij} in Ω_s and the microscopic displacement u_i, linearly depends on the two macroscopic loading parameters, namely, the macroscopic strain tensor ϵ_{ij} and the pore pressure p. According to equations (1.17) and (1.18), this property also holds for σ_{ij}. The most general linear macroscopic stress–strain relation thus is

$$\sigma_{ij} = C_{ijkl} \epsilon_{lk} - b_{ij} p \tag{1.19}$$

or alternatively

$$\epsilon_{ij} = S_{ijkl} \sigma_{lk} + \beta_{ij} p. \tag{1.20}$$

S_{ijkl} is the compliance tensor of the porous rock under drained conditions, and C_{ijkl} is the drained elastic stiffness tensor. In the isotropic case, b_{ij} reduces to $b \, \delta_{ij}$, where the scalar b is the Biot coefficient. In the general anisotropic case, the Biot coefficient indeed becomes a symmetric second-order tensor (see also the section on anisotropic poroelasticity).

Equation (1.19) introduces the effective stress tensor σ^{eff}_{ij}, which proves to control the macroscopic strain according to $\sigma^{eff}_{ij} = C_{ijkl} \epsilon_{lk}$.

We have seen that the solid domain Ω_s is always made up of the same microscopic particles. As far as the fluid is concerned, the external boundary S_{ff} of the fluid domain Ω_f at time t appears, according to equation (1.10a), as the image of S^0_{ff}. However, as opposed to the solid, this boundary condition is not of mechanical nature, insofar as it does not represent the actual displacement of the fluid phase. Indeed, the real transformation of the fluid is not relevant in this study in which the REV is regarded as an open system. Hence, equation (1.10a) is only a geometrical condition that aims at specifying the external boundary of the fluid particle constituting the REV at time t. Together with equation (1.10a), the determination of the current location of S_{sf}, which is gained through the resolution of the micromechanical problem in equations (1.10b) through (1.13), completely characterizes this fluid particle.

We have previously defined the normalized fluid volume v as the ratio of the fluid volume in the REV over the volume of the REV in the reference state, i.e., Ω^0. The variation $v - v_0$ is equal to the normalized flux of the displacement u_i through the boundary $S^0_{ff} \cup S^0_{sf}$:

$$v - v_0 = \frac{1}{\Omega^0}\left(\int_{S^0_{ff}} x_j \epsilon_{ij} n_i \, dS + \int_{S^0_{sf}} u_i n_i \, dS\right). \tag{1.21}$$

Again, we use the fact that the solution (u_i, s_{ij}) of equations (1.10b) through (1.13) linearly depends on ϵ_{ij} and p. Equation (1.21) shows that this property also holds for $v - v_0$, which thus can be put in the form

$$v - v_0 = b'_{ij}\epsilon_{ij} + \frac{p}{M}. \tag{1.22}$$

The displacement u_i is a priori only defined in the solid domain Ω^0_s, as well as on the boundary of Ω^0. Nevertheless, it is possible to extend the displacement to the fluid domain Ω^0_f so as to satisfy the boundary condition of equation (1.10a) and the continuity through S^0_{sf}. Such an extension is of course nonunique. However, an integration by parts on the fluid domain Ω^0_f is

$$\int_{\Omega^0_f} \frac{\partial u_i}{\partial x_j} \, d\Omega = \int_{\partial\Omega^0_f} u_i n_j \, dS = \int_{S^0_{ff}} n_j \epsilon_{ik} x_k \, dS + \int_{S^0_{sf}} u_i n_j \, dS. \tag{1.23}$$

We note that the right side in equation (1.23) is completely determined by the value of u_i on the fluid–solid interface, which in turn only depends on ϵ_{ij} and p. This means that the average strain over the fluid is unique, i.e., does not depend on the considered extension of the displacement to the fluid domain. Besides, for any extension complying with the above conditions, one obtains

$$\int_{\Omega_0} \frac{\partial u_i}{\partial x_j} \, d\Omega = \int_{\partial\Omega_0} u_i n_j \, dS = \int_{\partial\Omega_0} n_j \epsilon_{ik} x_k \, dS = \epsilon_{ij} \mid \Omega_0 \mid . \tag{1.24}$$

In other words, the average strain $<e_{ij}>$ over the whole REV is equal to the macroscopic strain tensor:

$$\epsilon_{ij} = <e_{ij}>. \tag{1.25}$$

Let us now consider the mechanical energy dw_s provided to the solid phase in the REV during an incremental loading $(d\epsilon_{ij}, dp)$. Denoting the corresponding incremental displacement by du_i,

$$dw_s = \int_{S^0_{ss}} du_i s_{ij} n_j \, dS - \int_{S^0_{sf}} p \, du_i n_i \, dS, \tag{1.26}$$

where n_i denotes the unit normal-oriented outward with respect to the solid. With the same reasoning as in equation (1.21), the increment dv of the normalized pore volume is the (normalized) flux of du_i through the boundary of the fluid:

$$dv = \frac{1}{\mid \Omega^0 \mid} \left(\int_{S^0_{sf}} du_i n_i \, dS + \int_{S^0_{ff}} du_i n_i \, dS \right), \tag{1.27}$$

where n_i now denotes the unit normal-oriented outward with respect to the fluid. Taking into account the normal orientation in the first integral of equation (1.27), which is the reverse of that in the second integral of equation (1.26), equations (1.26) and (1.27) yield

$$dw_s = \mid \Omega^0 \mid p \, dv + \int_{S^0_{ss}} du_i s_{ij} n_j \, dS - p \int_{S^0_{ff}} du_i n_i \, dS. \tag{1.28}$$

Taking equations (1.10) and (1.11) into account, we observe that equation (1.28) also is

$$\begin{aligned} dw_s &= \mid \Omega^0 \mid p \, dv + \int_{\partial \Omega^0} du_i s_{ij} n_j \, dS \\ &= \mid \Omega^0 \mid p \, dv + d\epsilon_{ik} \int_{\partial \Omega^0} x_k s_{ij} n_j \, dS \end{aligned} \tag{1.29}$$

Using equation (1.15) in equation (1.29) finally yields

$$dw_s = \mid \Omega^0 \mid \left(p \, dv + \sigma_{ij} d\epsilon_{ij} \right). \tag{1.30}$$

Neglecting any dissipative phenomenon, the mechanical work w_s supplied to the solid is stored in the form of elastic energy and, under isothermal conditions, can be identified to the free energy of the solid domain. In the framework of this micromechanical approach, w_s appears as a function of the macroscopic loading parameters ϵ_{ij} and p. Following Deudé et al. (2002), it is therefore convenient to introduce the potential energy of the solid phase $w^*_s = w_s - pv \mid \Omega^0 \mid$, which satisfies

$$dw^*_s = \mid \Omega^0 \mid \left(-v \, dp + \sigma_{ij} d\epsilon_{ij} \right) \tag{1.31}$$

The parameter w_s^* proves to be a potential for the poroelastic constitutive behavior, with the state variables ϵ_{ij} and p:

$$v = -\frac{1}{\mid \Omega^0 \mid}\frac{\partial w_s^*}{\partial p} \qquad \sigma_{ij} = \frac{1}{\mid \Omega^0 \mid}\frac{\partial w_s^*}{\partial \epsilon_{ij}}. \tag{1.32}$$

This property shows that the tensors b_{ij} in equation (1.19) and b'_{ij} in equation (1.22) are equal:

$$b_{ij} = -\frac{\partial \sigma_{ij}}{\partial p} = \frac{\partial v}{\partial \epsilon_{ij}} = b'_{ij}. \tag{1.33}$$

Drained and Undrained Descriptions

We return in the following to the macroscopic approach in the isotropic case. As stated above, the existence of a fluid phase in the connected porous space of the rock implies that two distinct descriptions have to be considered: the drained and undrained descriptions, associated repectively with the choice of either p or m as thermodynamic variable. Stress–strain relations in the *drained* description are identical to that of classical elasticity for nonporous solids, provided that effective pressure is substituted for the usual pressure. These relations can be summarized by the following expressions:

$$\varepsilon = -\frac{P_e}{K} \qquad \epsilon_{ij} = \frac{\left(\sigma_{ij}\right)_e}{2\mu}, \qquad i \neq j \tag{1.34}$$

or equivalently

$$\sigma_{ij} = \left(K - \frac{2\mu}{3}\right)\varepsilon\delta_{ij} + 2\mu\epsilon_{ij} - bp\delta_{ij}. \tag{1.35}$$

Another alternative form is

$$E\epsilon_{ij} = (1+\nu)(\sigma_{ij} + bp\delta_{ij}) - \nu(\sigma_{kk} + 3bp)\delta_{ij}, \tag{1.36}$$

where E is the Young modulus and ν the Poisson ratio. The above relations are to be understood as linear and isotropic relations between strains, stresses σ_{ij}, and fluid pressure p. Such strains can be realized through a two-step deformation process: a deformation due to applying σ_{ij} at constant zero fluid pressure, then a deformation due to applying fluid pressure p at constant σ_{ij}. Note that the theory involves at that point three elastic constants: K (drained bulk modulus), μ (shear modulus), and b (Biot coefficient). The shear strains are unaffected by the presence of a fluid because $\sigma_{ij}^{eff} = \sigma_{ij} (i \neq j)$. The existence of a fluid phase modifies the mechanical behavior of the rock only in the case of normal stresses. Because of the assumption of linearity, K and μ are considered to be independent of fluid pressure. In the *undrained* description, fluid pore pressure p is no longer an independent variable. The appropriate thermodynamic variable is the fluid mass content per unit

reference volume m. It is then convenient to define an undrained bulk modulus K_u so that the stress–strain relations in the undrained description can be written as

$$\varepsilon = -\frac{P}{K_u} \qquad \epsilon_{ij} = \frac{\sigma_{ij}}{2\mu}, \qquad i \neq j \tag{1.37}$$

or equivalently

$$\sigma_{ij} = \left(K_u - \frac{2\mu}{3}\right)\varepsilon\delta_{ij} + 2\mu\epsilon_{ij}. \tag{1.38}$$

Again, because the shear strains are unaffected by the existence of a fluid phase, the shear modulus is the same as in the drained case. It appears then that linear isothermal poroelastic theory involves four constants K, K_u, μ, and b. The preceding relations are to be understood as linear relations expressing strains as functions of a single set of variables, the stresses σ_{ij}. Although the above formulation is frequently used, it lacks the symmetry that one would expect compared with equation (1.35), where two sets of variables appear. The second variable should be in this case the mass content m so that a more symmetric and complete equation would express ϵ_{ij} as functions of σ_{ij} and m, exactly as equation (1.35) expresses ϵ_{ij} as functions of σ_{ij} and p. The fluid mass variation effect (following a first deformation step due to applying σ_{ij} at constant m) is not examined here but can easily be derived, as will be subsequently shown. Equations (1.37) and (1.38) are thus incomplete, but their complete form, including the mass variation effect, will be given later.

Fluid Pressure Variation in the Undrained Regime

In the undrained regime, i.e., deformation taking place at constant m, the fluid pressure varies. How can we calculate its variation? Using the stress–strain relations of equations (1.7) and (1.37) allows us to derive the expression for fluid pressure in the undrained regime:

$$p_u = -\frac{(K_u - K)\varepsilon}{b} = +BP, \tag{1.39}$$

where B is the Skempton coefficient:

$$B = \left(\frac{\partial p}{\partial P}\right)_m = \frac{(K_u - K)}{bK_u}. \tag{1.40}$$

B is the ratio of the pore pressure change (in the undrained regime) to the mean pressure change. Using the expression for b, one gets also $B = [(1 - K/K_u)/(1 - K/K_s)]$, which shows that B is a nondimensional parameter that varies between 0 (if $K \to K_u$, highly compressible fluid case) and 1 ($K \to 0$, very porous and compressible matrix case, or if $K_s \to K_f$, $K_u \to K_s$).

Fluid Mass Variation in the Drained Regime

Exactly as we have derived the relation giving the variation of pressure for an undrained deformation, we can derive the appropriate expression for the variation of mass in the case of drained deformation. In the case of drained deformation, m varies. How can $m - m_0$ be expressed in terms of the volumic strain ε and fluid pressure p? The answer is obtained by using the general Maxwell thermodynamics relations. Let $u_s(\epsilon_{ij}, v)$ be the internal energy of the solid phase per unit volume of porous rock. The internal energy u_s is the sum of several terms and will not be given explicitly at this point since we have chosen to derive the constitutive relations by starting from the linear stress–strain relations (an equivalent derivation would start from a quadratic expression for u_s). Obviously, for $v = 0$, the elastic part of u_s is the usual elastic energy $u_s(\epsilon_{ij}, 0) = u_s^0 + 1/2(K - 2\mu/3)\varepsilon^2 + \mu\epsilon_{ij}\epsilon_{ij}$. Introducing the first strain tensor invariant $I_1 = \varepsilon$ and the second strain tensor invariant $I_2 = \epsilon_{22}\epsilon_{33} + \epsilon_{33}\epsilon_{11} + \epsilon_{11}\epsilon_{22} - (\epsilon_{12})^2 - (\epsilon_{23})^2 - (\epsilon_{31})^2$, one can also write $u_s(\epsilon_{ij}, 0) = u_s^0 + 1/2(K + 4\mu/3)I_1^2 - 2\mu I_2$. Let us introduce the free energy per unit volume $\varphi_s(\epsilon_{ij}, p) = u_s - pv$. For an infinitesimal isothermal deformation,

$$d\varphi_s = \sigma_{ij}\, d\epsilon_{ij} - v\, dp. \tag{1.41}$$

But the fact that $d\varphi_s$ is a total differential implies that

$$\left(\frac{\partial \sigma_{ij}}{\partial p}\right)_{\epsilon_{ij}} = -\left(\frac{\partial v}{\partial \epsilon_{ij}}\right)_p = -\frac{1}{\rho_0}\left(\frac{\partial m}{\partial \epsilon_{ij}}\right)_p. \tag{1.42}$$

The previously established relations in equation (1.35) for stress–strain relations imply

$$\left(\frac{\partial \sigma_{ij}}{\partial p}\right)_{\epsilon_{ij}} = -b\delta_{ij}. \tag{1.43}$$

Combining the above results and recalling that we are within the framework of a linear theory, one can express $m - m_0$ as

$$m - m_0 = b\rho_0\varepsilon + \frac{p}{M'}, \tag{1.44}$$

where the constant M' is determined by the condition $m = m_0$ when the deformation is undrained and $p = BP$. M' is a Biot-Willis storage coefficient. Note that M' differs from the previous coefficient M by a quantity v_0/K_f. Thus

$$m - m_0 = b\rho_0\varepsilon + b^2\rho_0\frac{p}{(K_u - K)} = \frac{b\rho_0}{BK}(p - BP), \tag{1.45}$$

which is the desired relation. Equation (1.45) shows that b, defined in equation (1.8), is also given by

$$b = \left(\frac{\partial P}{\partial p}\right)_\varepsilon = \frac{1}{\rho_0}\left(\frac{\partial m}{\partial \varepsilon}\right)_p. \tag{1.46}$$

Equation (1.46) is a Maxwell relation corresponding to the thermodynamic potential $h_s(\varepsilon, p)$ such that $dh_s = Pd\varepsilon + (m/\rho_0)dp$. It expresses the equality of the second mixed derivatives of h_s. Extracting from equation (1.45) p as a function of m and P and utilizing equation (1.34) yields

$$\varepsilon = -\frac{P}{K_u} + B\frac{(m - m_0)}{\rho_0}, \tag{1.47}$$

which is the complete form of equation (1.37) when a two-step deformation is considered: a deformation due to applied stresses at constant m, and a deformation due to mass variation at constant stresses. Equation (1.47) shows that B, defined by equation (1.40), is also given by

$$B = \left(\frac{\partial p}{\partial P}\right)_m = \rho_0 \left(\frac{\partial \varepsilon}{\partial m}\right)_P. \tag{1.48}$$

Equation (1.48) is a Maxwell relation corresponding to the thermodynamic potential $g_s(P, m/\rho_0)$, such that $dg_s = \varepsilon\, dP + p(dm/\rho_0)$. It expresses the equality of the second mixed derivatives of g_s.

The apparent fluid volume fraction variation $v - v_0$ can easily be derived from the previous result with the use of $m - m_0 = \rho_0(v - v_0) + v_0(\rho - \rho_0)$, where the variation of ρ is $\rho - \rho_0 = \rho_0(p/K_f)$, introducing the fluid bulk modulus K_f. Because the rock is fluid saturated, $v_0 = \Phi_0$ and

$$v - v_0 = b\varepsilon + \left(\frac{b^2}{(K_u - K)} - \frac{\Phi_0}{K_f}\right) p. \tag{1.49}$$

Biot-Gassmann Equation

Equation (1.49) allows us to derive a general relation between both moduli K and K_u (Biot-Gassmann equation). A simple way to derive this relation is to consider the particular case where $p = P$. In such a situation, each point in the solid part of the rock is submitted to the same isotropic pressure P. Because of the homogeneous state of pressure in the porous saturated rock, the fluid phase could be replaced by the solid phase without any modification of the stress state. The medium behaves exactly as if it was composed of a single phase of bulk modulus K_s, so that $P = p = -K_s\varepsilon$. Moreover, $(v - v_0)/v_0 = \varepsilon$ and $v_0 = \Phi_0 = \Phi$, because the porosity remains constant in this case (homogeneous deformation). Equation (1.49) can then be written as

$$v - v_0 = \Phi_0\varepsilon = b\varepsilon + \left(\frac{b^2}{(K_u - K)} - \frac{\Phi_0}{K_f}\right)(-K_s\varepsilon). \tag{1.50}$$

This provides the Biot-Gassmann equation

$$K_u = K + \frac{b^2}{\frac{\Phi_0}{K_f} + \frac{(b-\Phi_0)}{K_s}} \tag{1.51}$$

or

$$\frac{1}{K} - \frac{1}{K_u} = \frac{\left(\frac{1}{K} - \frac{1}{K_s}\right)^2}{\frac{1}{K} - \frac{1}{K_s} + \Phi_0 \left(\frac{1}{K_f} - \frac{1}{K_s}\right)}. \tag{1.52}$$

As intuitively expected, when the fluid cannot flow out of the rock, the rock is stiffer, so that $K_u > K$. The Biot-Gassmann equation is a general relation between both the drained and undrained bulk moduli, which involves the bulk moduli of both the solid and fluid phases K_s and K_f together with porosity Φ_0. The Biot coefficient in equation (1.52) is expressed itself in terms of K and K_s from equation (1.8). Some extreme cases from equation (1.52) are of special interest. First, a very porous rock is expected to have a Biot coefficient b close to 1, since in that case, $K \ll K_s$. Consequently, $1/K_u \approx \Phi/K_f + (1 - \Phi)/K_s$ in that case. This is the harmonic average result. A second case of interest is that of a moderate-porosity rock saturated with a highly compressible fluid (a gas) such that $K_f \approx 0$. Then $K_u \approx K$. A strong variation is thus predicted for the undrained bulk modulus (and hence P-wave velocity) in the same rock when saturation switches from gas to liquid, a result of great importance in oil and gas exploration.

Fluid Diffusion at Macroscopic Scale

Both the drained and undrained deformation regimes refer to the deformation of a small volume in the medium. The considered volume is small in the previously defined sense: small compared with the macroscopic scale and yet large with respect to the microscopic scale. The fluid pressure is assumed here to vary at the macroscopic scale. Recall the expression of Darcy's law in the case where, as previously, p represents the perturbation of hydraulic pressure from hydrostatic equilibrium state:

$$q_i = -\frac{k}{\eta} \partial_i p, \tag{1.53}$$

where q_i is the ith component of the filtration velocity, k the rock permeability (assumed to be isotropic here), and η the fluid viscosity. Let us point out that the filtration velocity is not the local true fluid velocity within the pores. Darcy's law means that fluid flow will take place at the macroscopic scale as a consequence of fluid pressure gradient. This raises the following questions: what is the time constant for such a flow, and can we derive it from what we know? The mass conservation equation implies that

$$\partial_t m + \partial_i \rho q_i = 0 \tag{1.54}$$

Equations (1.53) and (1.54), together with equations (1.35) and (1.45) and the static mechanical equilibrium equation

$$\partial_j \sigma_{ij} = 0, \tag{1.55}$$

constitute the appropriate set to derive the fluid mass diffusion equation in the case of a linear and isotropic elastic behavior of the skeleton. As explained previously, stress, strain, and fluid pressure are defined as small perturbations from an equilibrium state so that the volumetric forces can be set to zero. Combining equations (1.55) and (1.35) yields

$$\partial_j \sigma_{ij} = 0 = \left(K + \frac{\mu}{3}\right) \partial_{ik} u_k + \mu \nabla^2 u_i - b\, \partial_i p, \tag{1.56}$$

where ∇^2 is the Laplacian operator. Taking the divergence of the above equation yields

$$\left(K + \frac{4\mu}{3}\right) \nabla^2 \partial_k u_k = b \nabla^2 p. \tag{1.57}$$

Combining equations (1.53) and (1.54), and assuming that the fluid compressibility is reasonably small, gives

$$\partial_t m = \rho \frac{k}{\eta} \nabla^2 p. \tag{1.58}$$

The approximation in the above relation is that the term $\partial_k \rho \partial_k p$ is negligible compared with $\rho \nabla^2 p$. A relation between m, p, and $\partial_k u_k$ can be obtained using the Laplacian of equation (1.45):

$$\nabla^2 m = b\rho \left(\nabla^2 \partial_k u_k + b \frac{\nabla^2 p}{(K_u - K)}\right). \tag{1.59}$$

Together with equation (1.57), the last equation gives

$$\left(K + \frac{4\mu}{3}\right)(K_u - K) \nabla^2 m = b^2 \rho \left(K_u + \frac{4\mu}{3}\right) \nabla^2 p, \tag{1.60}$$

and so from equation (1.58), the diffusion equation is found to be

$$\partial_t m = c\, \nabla^2 m, \tag{1.61}$$

where c is the hydraulic diffusivity. It follows from the above calculation that c is given by

$$c = \frac{B}{b} K_u \frac{k}{\eta} \frac{(K + \frac{4\mu}{3})}{(K_u + \frac{4\mu}{3})}. \tag{1.62}$$

Assuming both B and b to be of the order of unity, $\eta = 10^{-3}$ Pa·s (water at room conditions), $k = 10^{-15} m^2$ (1 mDarcy), $K_u = 20$ GPa, and with the approximation that $(K + 4\mu/3)/(K_u + 4\mu/3)$ is close to 1, one obtains $c \approx 2.10^{-2} m^2 s^{-1}$. The solutions of the diffusion equation are such that the time constant τ for fluid to diffuse over a distance L is $\tau \approx L^2/c$. Fluid diffusion is a slow process since $\tau \approx 150$ years for $L = 10$ km. It is of interest to note that, although the equation

governing the fluid-mass evolution is a diffusion equation, the equation governing the fluid pressure is in general more complicated. Use of equations (1.45) and (1.58) leads to

$$\rho \frac{k}{\eta} \nabla^2 p = b\rho \, \partial_t \varepsilon + b^2 \frac{\rho}{(K_u - K)} \, \partial_t p, \tag{1.63}$$

which contains the term $b\rho \, \partial_t \varepsilon$ in addition to the diffusion equation terms.

Fluid Flow at Microscopic Scale

As a macroscopic theory, poroelastic theory considers the rock as an idealized continuous medium. As discussed previously, this can be reconciled with a microscopic approach if all defined mechanical quantities are averaged over spatial and temporal scales large compared with those of the microscopic process, which are thus in general ignored. We come back in this subsection to the microscopic point of view because there are some important microscopic processes that cannot be ignored. Up to now, we have assumed that fluid pressure p is constant everywhere within the REV. This key assumption of poroelasticity is violated in a particular case that is important. The microscopic process involved is the so-called squirt-flow mechanism (Dvorkin et al., 1994). The variable stresses caused by the propagation of an elastic wave in a porous saturated rock induce pore pressure gradients on the scale of individual pores. Equant pores are stiff and flat pores are compliant. A high compressive stress at the microscopic pore scale will expel fluid from compliant pores (where fluid pressure is high) toward stiff pores (where it remains low). This process takes place at the pore scale and dissipates energy. At high frequencies (for instance, ultrasonic frequencies in laboratory), the elastic wave period is so short that the fluid has no time to move. The medium behaves then as a two-phase medium, the solid and fluid phases being both immobile. This situation corresponds to a variable fluid pressure from pore to pore. It cannot be handled by using poroelasticity. EMT is the appropriate tool in that case to derive the values of the "high frequency" effective elastic moduli (Guéguen and Palciauskas, 1994; Le Ravalec and Guéguen, 1994) K_{hf} and μ_{hf}. EMT allows one to express these moduli in terms of the solid- and fluid-phase moduli, the porosity Φ_0, and the pore shape parameters (such as the pore aspect ratio A, which is defined as the ratio of the crack aperture to the crack length). What is meant by high frequency remains to be specified. The characteristic angular frequency ω_c is given by

$$\omega_c = A^3 \frac{K}{\eta}. \tag{1.64}$$

At frequencies $\omega \gg \omega_c$, the fluid has no time to move. For $\omega \ll \omega_c$, local fluid flow takes place at the microscopic pore scale (squirt flow). Typically, if $K = 20$ GPa, $\eta = 10^{-3}$ Pa·s, and $A \approx 10^{-3}$ (A is the crack aspect ratio), $\omega_c \approx 20$ kHz. As a result, dispersion of elastic waves is expected. High velocity values are predicted at $\omega \gg \omega_c$, and low velocity values at $\omega \ll \omega_c$. This

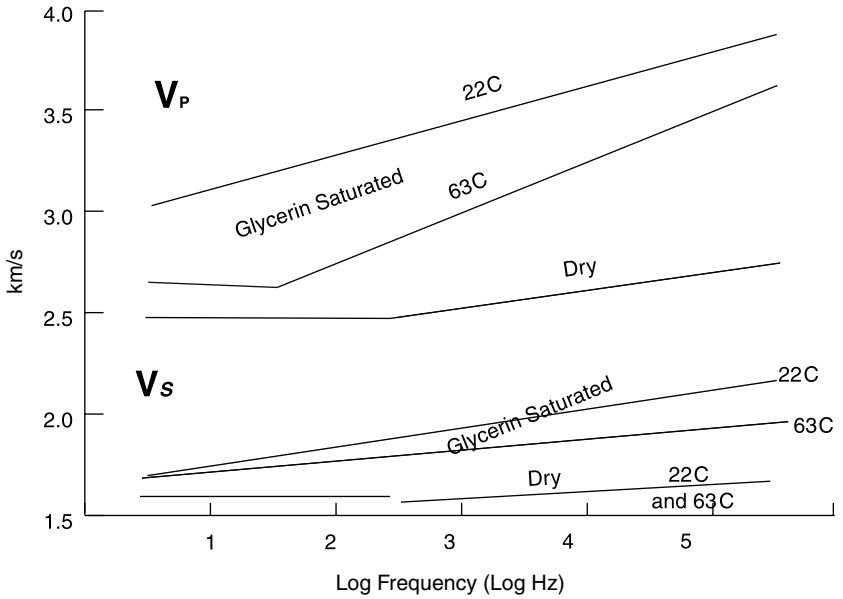

Figure 1.3 ► Compressional and shear wave velocity versus frequency for a dry and glycerine-saturated sandstone. Velocities are measured at 22°C and 63°C, effective pressure is 17 MPa (Upper Fox Hills sandstone, from Batzle, 2001).

is confirmed by laboratory results (Batzle et al., 2001) for both the frequency dependence and the viscosity dependence of ω_c (Figure 1.3). Combining linear poroelasticity and EMT makes it possible to predict the high- and low-frequency velocities (Le Ravalec and Guéguen, 1996). At high frequencies, the bulk and shear moduli K_{hf} and μ_{hf} are obtained from a micro model using EMT only. At low frequencies, the bulk and shear moduli K_{lf} and μ_{lf} are obtained from the Biot-Gassmann equation (1.51), because the low-frequency moduli are identical to the undrained moduli: at low frequencies, an isobaric state is reached at the scale of the REV, the scale at which p is defined. Equation (1.51) provides the theoretical bulk modulus value if K, μ, K_f, K_s, and Φ_0 are known. The values of the drained moduli K and μ can be derived independently from EMT: they correspond to the effective moduli of a solid medium with empty pores. This results from the linearity assumption, implying that fluid pressure dependence of K and μ is neglected. Consequently, K and μ depend on K_s, Φ_0, and pore shape parameters (such as the pore aspect ratio A). The EMT calculation giving these moduli is exactly similar to that giving K_{hf} and μ_{hf}, the only difference being that in the former case pores are considered to be empty whereas in the latter they are considered to be fluid saturated. Although we do not consider in this chapter the dynamic poroelastic theory, the preceding remarks allow us to conclude that high and low elastic-wave velocities are different. This means that ultrasonic measurements in the megahertz range in the laboratory should not be used to interpret

seismological data recorded in the hertz range. Dynamic poroelasticity is out of the scope of this book. It takes into account the inertia effects, which become important in a frequency range that is much higher than the critical value ω_c.

1.2.2 Linear Nonisothermal Poroelasticity

Nonisothermal porous media are encountered in numerous cases. Nuclear waste disposal is an important example for low-porosity rocks. Oil recovery in deep rock reservoirs and frictional heating in fault zones are two other very different examples of interest. The extension of the previous theoretical framework to nonisothermal deformation is straightforward (Palciauskas and Domenico, 1982; McTigue, 1986). It requires the introduction of the thermal expansivities of the fluid, bulk and pore volumes, and modified constitutive relations.

Drained Deformation: Constitutive Relations and Fluid Mass Variation

Let T_0 be a reference temperature, and consider a possible temperature change $T - T_0$. This will result in a thermal expansion of the rock, so that an additional deformation has to be accounted for. This is expressed by the following equation, which has to be used instead of equation (1.34) for drained deformation:

$$\varepsilon = -\frac{P_e}{K} + \alpha_b (T - T_0), \tag{1.65}$$

where α_b is the bulk drained thermal expansivity of the porous rock:

$$\alpha_b = \frac{1}{V}\left(\frac{\partial V}{\partial T}\right)_{P,p}. \tag{1.66}$$

In the drained regime, equation (1.45), which expresses the fluid mass variation in the isothermal case, is to be modified as follows:

$$m - m_0 = \left(\frac{b\rho_0}{BK}\right)(p - BP) + m_0\, \alpha_m\, (T - T_0), \tag{1.67}$$

where the thermal expansion coefficient α_m, which reflects changes in the fluid mass content at constant mean pressure P and fluid pressure p, is defined as

$$\alpha_m = \frac{1}{m}\left(\frac{\partial m}{\partial T}\right)_{P,p}. \tag{1.68}$$

Given that $m = \rho\Phi$, and using equation (1.68), it follows that

$$\alpha_m = \frac{1}{\rho}\left(\frac{\partial \rho}{\partial T}\right)_{P,p} + \frac{1}{\Phi}\left(\frac{\partial \Phi}{\partial T}\right)_{P,p} = \alpha_\Phi - \alpha_f, \tag{1.69}$$

where $\alpha_f = -1/\rho\,(\partial\rho/\partial T)_{P,p}$ is the fluid thermal expansivity and $\alpha_\Phi = 1/\Phi\,(\partial\Phi/\partial T)_{P,p}$ is the pore thermal expansivity. For water at room pressure and temperatures below 80°C, $\alpha_f \approx 5.10^{-4}C^{-1}$ so that in general $\alpha_\Phi \ll \alpha_f$ and α_m is negative: when temperature increases, the fluid mass decreases. Substituting equation (1.65) in equation (1.67), it is possible to express the fluid mass variation in terms of ε, p, and T:

$$m - m_0 = -b\rho_0\varepsilon + \frac{b\rho_0 p}{BK_u} + (\Phi\,\alpha_m - b\,\alpha_b)\rho_0(T - T_0). \tag{1.70}$$

From this last equation, the temperature dependence of the fluid mass is, at constant ε and p,

$$\left(\frac{\partial m}{\partial T}\right)_{\varepsilon,p} = (\Phi\,\alpha_m - b\,\alpha_b)\,\rho_0\,(T - T_0). \tag{1.71}$$

The sign of this coefficient is in general negative.

Undrained Deformation: Constitutive Relations and Fluid Pressure Variation

In the undrained regime, equation (1.37) is modified to account for thermal expansion as follows:

$$\varepsilon = -\frac{P}{K_u} + \alpha_u\,(T - T_0), \tag{1.72}$$

where α_u is the bulk undrained thermal expansivity of the porous rock. In the undrained regime, fluid mass is constant, so that from equation (1.67)

$$m - m_0 = \left(\frac{b\rho_0}{BK}\right)\,(p - BP) + m_0\,\alpha_m\,(T - T_0) = 0. \tag{1.73}$$

Equivalently, equation (1.73) can be written as a generalization of the Skempton coefficient definition:

$$p_u = B[P - K\frac{\Phi_0}{b}\alpha_m(T - T_0)]. \tag{1.74}$$

This allows us to calculate how fluid pressure varies when temperature increases at constant pressure P:

$$\left(\frac{\partial p}{\partial T}\right)_{m,P} = -\alpha_m\,\Phi_0\,K\frac{B}{b}. \tag{1.75}$$

As discussed previously, α_m is in general negative so that the fluid pressure increases with temperature: $(\partial p/\partial T)_{m,P} \geq 0$. The value of this coefficient was

calculated to be $0.7 \times 10^5 Pa \cdot C^{-1}$ by Le Ravalec and Guéguen (1994) for a granitic rock with $\alpha_m = -46 \times 10^{-5}\ C^{-1}$, $\Phi_0 = 0.18 \times 10^{-2}$, $K = 27$ GPa, $B = 0.9$, $b = 0.3$. Using equation (1.70) allows us similarly to calculate how fluid pressure varies when temperature increases at constant bulk volume:

$$\left(\frac{\partial p}{\partial T}\right)_{\varepsilon, P} = (b\ \alpha_b - \Phi\ \alpha_m)\ K_u \frac{B}{b}. \tag{1.76}$$

Again, fluid pressure increases with temperature since $(\partial p/\partial T)_{\varepsilon, P} > 0$. Using the same reference values as above, with $\alpha_b = 5 \times 10^{-5} C^{-1}$, $K_u = 38$ GPa, one gets $(\partial p/\partial T)_{\varepsilon, P} = 12.8 \times 10^5\ Pa \cdot C^{-1}$. These results show that a significant fluid pressure increase is to be expected in a low permeability rock if thermal heating is assumed to take place in the undrained regime. A possible case where this could apply is the underground storage of nuclear waste in a granitic rock.

Drained and Undrained Thermal Expansion Coefficients

Several thermal expansion coefficients have been introduced in the previous sections. The porous rock has two thermal expansion coefficients, α_b and α_u. A simple relation between both can be derived as follows. From equations (1.65) and (1.72), considering the undrained regime where p_u is given by equation (1.74),

$$\varepsilon = -\frac{P - bp_u}{K} + \alpha_b(T - T_0) = -\frac{P}{K_u} + \alpha_u(T - T_0). \tag{1.77}$$

Together with equation (1.74), equation (1.77) leads to

$$\alpha_u = \alpha_b - B\alpha_m \Phi. \tag{1.78}$$

Given that in most cases α_m is negative, in general it is the case that $\alpha_u > \alpha_b$.

1.2.3 Nonlinear Poroelasticity

It may happen that, in some cases, a porous rock exhibits a materially nonlinear behavior in the elastic domain. In the following we consider only isothermal conditions. This type of behavior can be accounted for from both the microscopic and macroscopic points of view. At the microscopic level, the origin of nonlinearity can be specified and analyzed as shown later. At the macroscopic level, the elastic free energy has to be expressed to a higher order in terms of strains (or stresses). This is similar to what is done in the case of nonlinear elasticity for nonporous rocks and minerals: third-order or even fourth-order terms are retained in the development of

the free energy, depending on their relative importance with respect to the quadratic term of linear elasticity.

Experimental Characterization of Nonlinearity

The nonlinear character of the rock response can be investigated by performing drained isotropic compressive tests. The macroscopic stress applied to the sample has the form $\sigma_{ij} = -P\delta_{ij}$, and the pore pressure is maintained at the constant value p. The confining pressure P, initially identical to the pore pressure p, is gradually increased (Figure1.4). The evolution of the volumetric strain in terms of the confining pressure reveals some aspects of the nonlinear response. Following

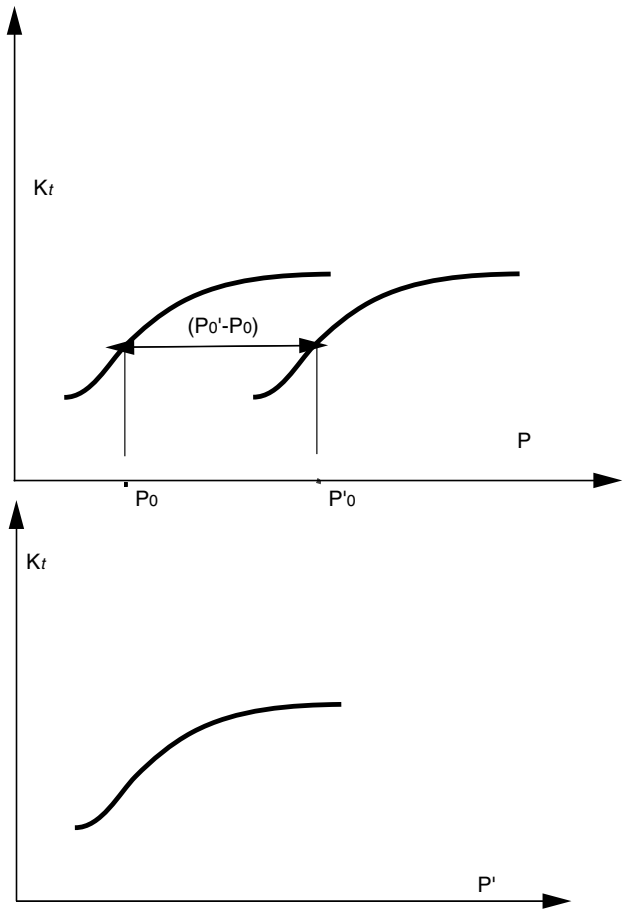

Figure 1.4 ► Tangent modulus. Two sets of experiments at different pore fluid pressures. In terms of the effective (Terzaghi) pressure P′, both sets are identical.

Boutéca et al. (1994), the nonlinear response is quantified in terms of a drained tangent bulk modulus defined as

$$\frac{1}{K_t} = -\frac{1}{V}\left(\frac{\partial V}{\partial P}\right)_p . \tag{1.79}$$

Experimental results show that K_t is an increasing function of P. It is also a function of p. For some rocks, the following observations were made. Considering two different values of the pore pressure, the corresponding curves $K_t(P)$ are shifted from each other along the axis of confining pressure by a quantity precisely equal to the difference in pore pressure (Figure1.4), (see also Zimmerman (1991)). For such rocks, K_t is a function of P and p through $P' = P - p$, which is commonly referred to as the Terzaghi effective pressure.

Microscopic Origin of Nonlinearity

For granular rocks such as sandstones, it has been argued that the nonlinearity could be attributed to the contact between two elastic grains, which is classically modeled as a Hertzian contact. A second possible origin of the nonlinearity is the presence of microcracks in the solid phase. Indeed, let us recall that, in general, the porous space comprises a set of cracks and a network of connected pores. In rocks such as sandstones, the contribution of cracks to the total porosity is in general negligible. However, the effect of cracks on the overall reponse can be significant. In both cases, Hertzian contacts or cracks, we can expect that the mechanical response will exhibit path dependence. Therefore in general, the deformation history must be explicitly known. This will be true at least for any stress state with a shear component. The case of isotropic compression could possibly exhibit no path dependence and correspond to a truly nonlinear elastic behavior. We shall consider in the following the special case in which the nonlinear macroscopic behavior is due to the closure of cracks induced by the confining (isotropic) pressure. This process is assumed to be nonlinear and elastic. Following these assumptions, the asymptotic regime of the $K_t(P)$ plot is related to the fact that all cracks are closed at sufficiently large confining pressures (Figure1.4). The asymptotic value of K_t is identical to that of the bulk modulus of the crack-free porous rock. Although the evolution of cracks is an important factor, that of pores is not because their shapes and volumes remain almost constant. Pores are supposed to be connected to each other and to be fluid saturated at pressure p. To clarify the issue of the connection between pores and cracks, a simple experiment can be made. The pore pressure and the confining pressure are maintained at identical values and are increased simultaneously from the initial values $p = 0$ and $P = 0$ to $p = P$. Then the volumetric strain and the fluid pressure variation are related by $\delta V/V = -\delta p/K_s$, where K_s is the apparent tangent modulus. If cracks are all connected to pores,

the solid phase undergoes a hydrostatic loading. Then stresses and strains are uniform and K_s is the bulk modulus of the solid phase. This result agrees with the measurements of Boutéca et al. (1994) on two different sandstones, showing a K_s value close to 35 GPa that was insensitive to p in the range from $p = 0$ to 100 MPa.

Macroscopic Constitutive Response

We examine nonlinear poroelasticity within the framework of the Biot (1973) semilinear theory of fluid-saturated porous solids. As before, the rock is assumed to be a homogeneous isotropic solid, saturated with a viscous compressible fluid. What are the stress–strain relations and what is the fluid mass expression in the nonlinear case? To answer that question, we extend in the following the previous relations obtained in the linear case.

Exactly as we introduced a stress decomposition to define an effective stress in equation (1.9), let us assume that the elastic deformation of a rock sample submitted to a stress $-P\delta_{ij}$ on its external surface and a fluid pressure p within the pores can be obtained by superimposing two states of equilibrium (Figure1.5). Isotropic compression is the only case examined here, for reasons previously discussed.

The first stress state corresponds to a stress $-(P-p)\delta_{ij}$ applied to the external surface of the rock and a zero fluid pressure within the pores. The second one is that of the same rock sample submitted to a pressure p on both the external surface of the rock and the internal surfaces of the pores.

The concept of semilinearity stipulates that the strains due to the first state, ϵ_1, involve nonlinear modifications of local geometries, such as crack closure, that affect the global nonlinear response of the matrix. We examine in the following how these assumptions modify the mechanical response, primarily the stress–strain relations. For reasons explained in the previous section, only the case of

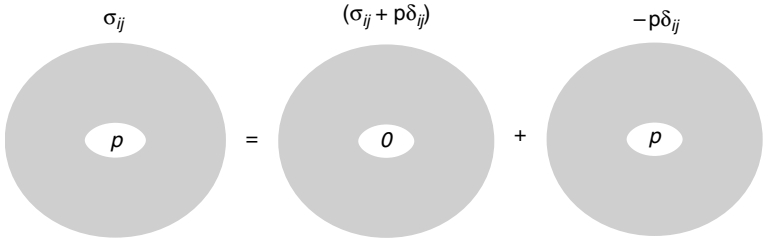

Figure 1.5 ► Stress decomposition for Biot semilinear model. The decomposition generalizes that described by Figure 1.1: the stress state is obtained by superimposing: (1) a stress $\sigma_{ij} + p\delta_{ij}$ on the external surface and a zero pressure in the pores, and (2) a compressive stress $-p\delta_{ij}$ on the external surface and in the pores.

isotropic compression is investigated. Then the strains due to the second state, ϵ_2, are assumed to be linear in p. This implies

$$\varepsilon_2 = -\frac{p}{K_s}. \tag{1.80}$$

The concept of semilinearity assumes that the total strain is obtained by superimposing both strains ε_1 and ε_2. Experimentally, as shown in Figure1.6, this assumption is excellent in many cases. We have

$$\varepsilon = \varepsilon_1 - \frac{p}{K_s}. \tag{1.81}$$

The strain ε_1 is the nonlinear part of the total strain, and it does not involve the fluid pore pressure within the rock because it corresponds to a stress applied only on the external rock surface (Figure1.5). In that case the rock is "drained" under a constant (zero) fluid pressure and its elastic nonlinear behavior can be described by a free energy f such that

$$P_1 = (P - p) = -\frac{\partial f}{\partial \varepsilon_1}, \tag{1.82}$$

where f refers to the "drained rock" at zero fluid pressure and is

$$f = f_2 + f_3, \tag{1.83}$$

where f_2 is the usual quadratic term. At constant temperature and for a drained rock,

$$f_2 = f_0 + \frac{1}{2}\left(K + \frac{4\mu}{3}\right) I_1^2 - 2\mu\ I_2, \tag{1.84}$$

where I_1 and I_2 are respectively the first and second strain invariants introduced earlier to calculate the fluid mass variation in equation (1.45). Then equations (1.82), (1.83), and (1.84) lead directly to the following stress–strain relation in the drained regime:

$$P = -K\varepsilon + bp - \frac{\partial f_3}{\partial \varepsilon_1}, \tag{1.85}$$

where the Biot coefficient is as before $b = 1 - (K/K_s)$. The first two terms of equation (1.85) are of course those previously found in the case of linear elasticity. The third-order term depends on f_3 and is a new term to the nonlinearity. It is a function of I_1, I_2, and the third strain invariant I_3. Because the rock is homogeneous and isotropic, f_3 is necessarily a function of only the strain invariants. Three combinations of the three strain invariants (I_1^3, $I_1 I_2$, I_3) can result in a cubic expression so that the third-order term normally leads to the introduction of three additional elastic constants. However, in the simple case of isotropic compression, $I_2 = I_1^2/3$ and $I_3 = (I_1/3)^3$, so that only one additional constant is needed. Then one can write

$$f_3 = \frac{d}{3} I_1^3. \tag{1.86}$$

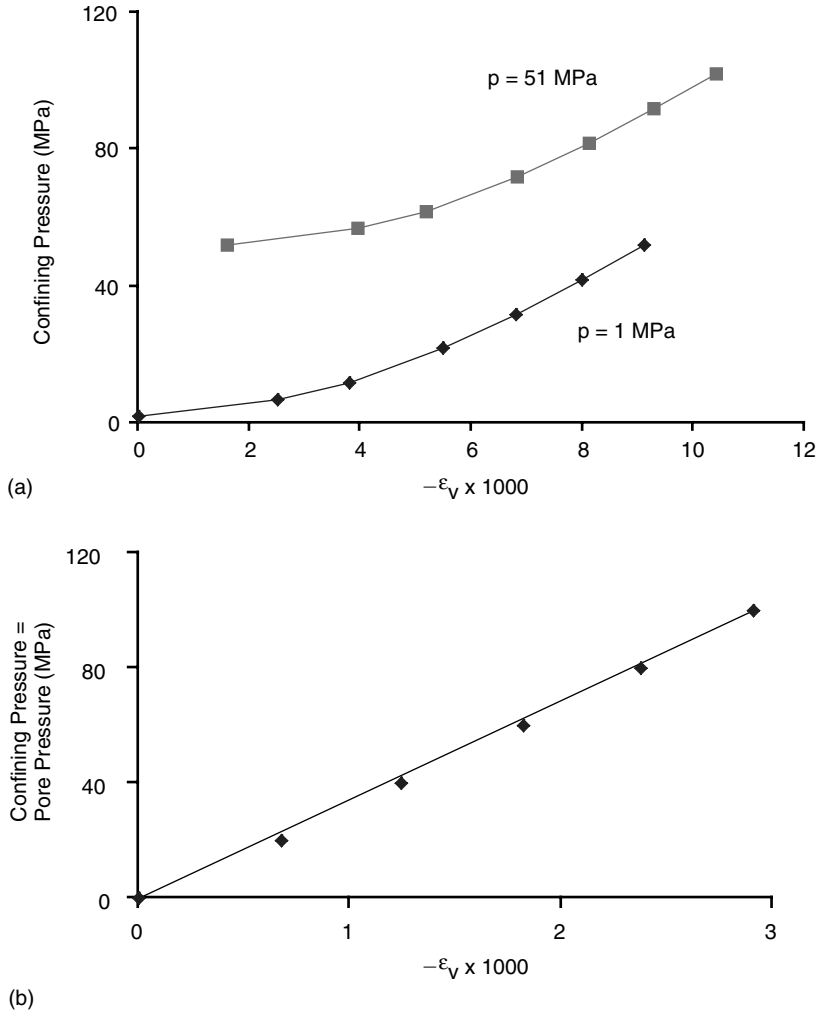

Figure 1.6 ► (a) Volumetric strain as a function of the isotropic loading (pressure applied on the external rock surface) at two given pore pressure levels (1 MPa and 51 MPa): a nonlinear behavior is clearly evidenced. (b) Volumetric strain for a loading path where the pressure applied on the external surface and the pore pressure are identical: a linear behavior is clearly evidenced, in agreement with the semilinear theory. (After Boutéca et al., 1994.)

Note that, at this level of analysis, nothing can be stated about d. Only from a microscopic analysis, for instance, with a specific model of elastic crack closure, would it be possible to specify d. Equations (1.81), (1.82), and (1.86) allow us to derive the complete stress–strain relations. Calculating the derivative of f_3 with

respect to the volumetric strain (which is equal to I_1), we get

$$\frac{\partial f_3}{\partial I_1} = d\ I_1^2. \tag{1.87}$$

The final stress–strain relation is

$$P = -K\varepsilon + bp - d(\varepsilon + \frac{p}{K_s})^2. \tag{1.88}$$

Let us now consider also the relation giving the fluid mass variation. In the drained regime, there is a fluid mass variation that can be obtained using the same method as in previous sections, adding the fluid mass variations of both stress states. For the second stress state, the strain is linear in fluid pressure, and

$$(m - m_0)_2 = \rho_0\ (v - v_0) + v_0\ (\rho - \rho_0), \tag{1.89}$$

where the variation of v in that case is $(v - v_0)/v_0 = \varepsilon = -p/K_s$ (homogeneous deformation, constant porosity). Because the rock is fluid saturated, $v_0 = \Phi_0$. Moreover, $(\rho - \rho_0)/\rho_0 = p/K_f$. Therefore

$$\frac{(m - m_0)_2}{\rho_0} = p\ \Phi_0\ \left(\frac{1}{K_f} - \frac{1}{K_s}\right). \tag{1.90}$$

For the first stress state, recall that the pore fluid pressure is constant (zero), so that the fluid mass variation results only from the porosity change. From $v = V_p/V_0$ and $V_p = V - V_s$, where V_p is the pore volume and V_s is the volume of solid phase in a rock volume V (V_0 is the initial value of V), one can derive $(v - v_0)_1 = (m - m_0)_1/\rho_0 = \varepsilon - (1 - \Phi_0)\varepsilon_s$. The strain ε_s is defined as the volumic strain in the solid phase. Introducing σ_s, the sum of the three diagonal components of the stress tensor in the solid phase, $\varepsilon_s = \sigma_s/3K_s$. Because the first stress state corresponds to an externally applied stress on a rock of porosity Φ_0 and zero fluid pressure, σ_s is related to P by a simple relation: $-P = (1 - \Phi_0)\sigma_s/3$. This leads to

$$\frac{(m - m_0)_1}{\rho_0} = \varepsilon + \frac{P}{K_s}. \tag{1.91}$$

Adding equations (1.90) and (1.91) and deriving P from equation (1.88), one gets

$$\frac{(m - m_0)}{\rho_0} = b\ \varepsilon + p\ \left(\frac{\Phi_0}{K_f} + \frac{(b - \Phi_0)}{K_s}\right) - \frac{d}{K_s}\ \left(\varepsilon + \frac{p}{K_s}\right)^2. \tag{1.92}$$

This shows that in the nonlinear case the Biot coefficient is modified by an additional term. The constitutive relations derived for the nonlinear case contain implicitly an effective pressure. The effective pressure law has not been given, however, and its exact value depends on the d value. In turn, the d value can only

be derived from a specific microscopic model. Using equation (1.79), it is easy to derive

$$K_t = K + 2d(\varepsilon + p\ K_s). \tag{1.93}$$

This shows that the tangent modulus differs between two experiments at different p values, p_1 and p_2, by the quantity $2d(p_2 - p_1)K_s$. This means that the constant d can be measured directly from $K_t - \varepsilon$ plots for different p values.

1.2.4 Anisotropic Linear Poroelasticity

Most rocks are anisotropic, although their anisotropy remains small in most cases. Constitutive equations for anisotropic poroelastic rocks have been studied by Brown and Korringa (1974), Carroll (1979), Thompson and Willis (1991), and Lehner (1997). Two main origins of rock anisotropy are the preferred orientation of grains and the alignment of cracks. The extension of poroelastic theory to the general anisotropic case can be viewed as an extension of anisotropic elasticity to porous media, similar to the extension of isotropic elasticity presented in the preceding sections.

Constitutive Relations

Linear stress–strain relations that generalize equation (1.35) can be written as

$$\sigma_{ij} = C_{ijkl}\ \epsilon_{kl} - b_{ij}\ p, \tag{1.94}$$

where C_{ijkl} is the drained elastic stiffnesses tensor. This fourth-order tensor follows the same symmetry rules as the usual elastic stiffnesses tensor. It can be represented by a 6×6 matrix using Voigt notation. The same is true for its inverse, the drained compliances tensor S_{ijkl}. The second-order tensor b_{ij} generalizes the Biot coefficient b. The quantity

$$\sigma_{ij}^{eff} = \sigma_{ij} + b_{ij}\ p \tag{1.95}$$

is an appropriate generalization of the Biot-Willis effective stress, and the existence of an effective stress principle in that case is a necessary consequence of linearization alone. A second linear relation provides a generalization of equation (1.49):

$$v - v_0 = b_{ij}\ \epsilon_{ij} + \frac{p}{M}. \tag{1.96}$$

Because $\left(\partial\sigma_{ij}/\partial p\right)_{\epsilon_{ij}} = -\left(\partial v/\partial\epsilon_{ij}\right)_p$ is still applicable, the same tensor b_{ij} appears in both equations (1.94) and (1.96) and is symmetric. Similar results can be derived for the undrained deformation regime, generalizing equation (1.47):

$$\epsilon_{ij} = (S_{ijkl})_u\ \sigma_{kl} + B_{ij}\ \frac{(m - m_0)}{\rho_0}, \tag{1.97}$$

where $(S_{ijkl})_u$ is the fourth-order tensor of undrained compliances, and B_{ij} is a second-order tensor that is equivalent to the Skempton coefficient in the isotropic case. The symmetry rules for the drained stiffnesses and compliances tensors are also applicable to the undrained ones. Moreover, B_{ij} is symmetric, as is b_{ij}.

Anisotropic Extension of Biot-Gassmann Equation

The Biot-Gassmann equation (1.51) or (1.52) provides a useful relation between both bulk moduli, drained and undrained, in terms of the solid-phase bulk modulus K_s, the fluid-phase bulk modulus K_f and the rock porosity Φ. This relation is independent of the pore shape geometry. As previously discussed, combining this relation with additional assumptions relative to pore shape geometry and using EMT allows calculation of the high- and low-frequency moduli. Extending this calculation to the anisotropic case provides similarly some interesting results on high- and low-frequency elastic stiffnesses or compliances. Brown and Korringa (1974) extended the Biot-Gassmann equation to anisotropic media. We give in the following their result in the case where the solid part of the rock is homogeneous (microscopic homogeneity). This is the same assumption we previously followed for isotropic rocks. As they have shown, if this condition is not met, a slightly more complex relation is found. Let us introduce the compliances tensor of the solid part of the rock $(S_{ijkl})_s$. The desired relation can be derived from first principles by considering an undrained regime and applying a stress change $\delta\sigma_{ij}$. Again this process can be described in two stages. Let us define δp, the pore pressure change resulting from the application of $\delta\sigma_{ij}$ in an undrained regime. Then we first apply on the external rock surface $\delta(\sigma_{ij})_1 = \delta\sigma_{ij} + \delta p\delta_{ij}$, in a drained regime (at constant pore pressure). In a second stage, we apply a stress $\delta(\sigma_{ij})_2 = -\delta p\delta_{ij}$ on the external surface and a pore fluid pressure δp within the pores (Figure 1.7). The overall strain variation $(S_{ijkl})_u\delta\sigma_{kl}$ is the sum of the two strains obtained in the two stages. The strain associated with the first stage is $(\delta\epsilon_{ij})_1 = S_{ijkl}(\delta\sigma_{kl} + \delta p\delta_{kl})$ and that associated with the second stage is $(\delta\epsilon_{ij})_2 = -(S_{ijkk})_s\delta p$. This provides the relation

$$\left[(S_{ijkl})_u - S_{ijkl}\right]\delta\sigma_{kl} = \left[S_{ijkk} - (S_{ijkk})_s\right]\ \delta p. \tag{1.98}$$

A second relation between $\delta\sigma_{ij}$ and δp can be obtained by requiring that the amount of fluid is conserved:

$$\delta V_p = -\frac{\delta p}{K_f}\ V_p = \left(\frac{\partial V_p}{\partial\sigma_{ij}}\right)_p (\delta\sigma_{ij})_1 + \left(\frac{\partial V_p}{\partial p}\right)_{(P-p)} \delta p, \tag{1.99}$$

where V_p is the pore volume in the rock volume V and $\Phi = V_p/V$. The last term in equation (1.99) represents the pore volume variation at constant differential pressure, i.e., for an identical pressure variation applied to both the external rock surface and the internal pore surfaces. As we have seen earlier in this chapter,

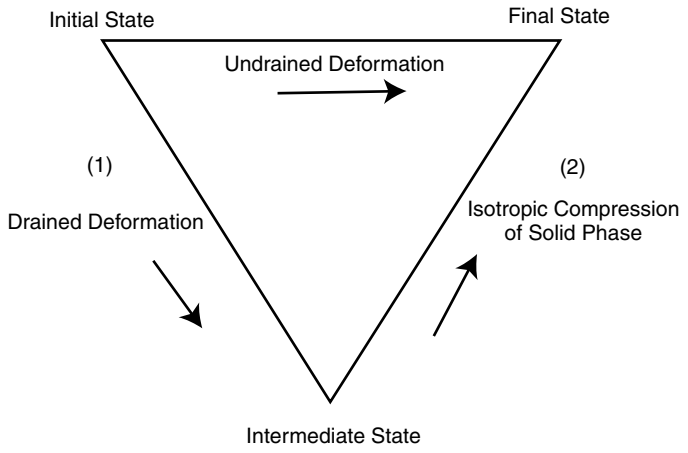

Figure 1.7 ► Undrained deformation of a sample submitted to an external stress variation $\delta\sigma_{ij}$ and a pore pressure variation δp in two steps corresponding to: (1) a drained deformation, and (2) an isotropic compression of the solid phase.

$1/K_\Phi = -1/V_p \left(\partial V_p/\partial p\right)_{(P-p)}$, with $K_\Phi = K_s$, because of the assumption of homogeneity of the solid phase. Then

$$\frac{\delta p}{K_f} = -\frac{1}{V_p}\left(\frac{\partial V_p}{\partial \sigma_{ij}}\right)_p \left(\delta\sigma_{ij}\right)_1 + \frac{1}{K_s}\,\delta p. \tag{1.100}$$

Defining $S'_{ij} = (1/V_p)\left(\partial V_p/\partial\sigma_{ij}\right)_p$ and substituting the $\delta(\sigma_{ij})_1$ value, one gets

$$-S'_{ij}\,\delta\sigma_{ij} = \delta p\left(\frac{1}{K_f} - \frac{1}{K_s} + S'_{kk}\right). \tag{1.101}$$

Then combining equations (1.98) and (1.101), we obtain the relation

$$S_{ijkl} - (S_{ijkl})_u = \left[S_{ijmm} - (S_{ijnn})_s\right] S'_{kl}\left(\frac{1}{K_f} - \frac{1}{K_s} + S'_{pp}\right)^{-1}. \tag{1.102}$$

To express S'_{kl} in terms of other known quantities, we use first the Maxwell relation associated with the potential Φ, such that $d\Phi = -\epsilon_{ij}d\sigma_{ij} - (V_p/V_0)dp$. This implies $(\partial\epsilon_{ij}/\partial p)_{\sigma_{ij}} = (1/V_0)(\partial V_p/\partial\sigma_{ij})_p$ or, substituting the definition of S'_{ij}, $(\partial\epsilon_{ij}/\partial p)_{\sigma_{ij}} = \Phi_0\ S'_{ij}$. Finally, the quantity $(\partial\epsilon_{ij}/\partial p)_{\sigma_{ij}}$ is obtained by considering

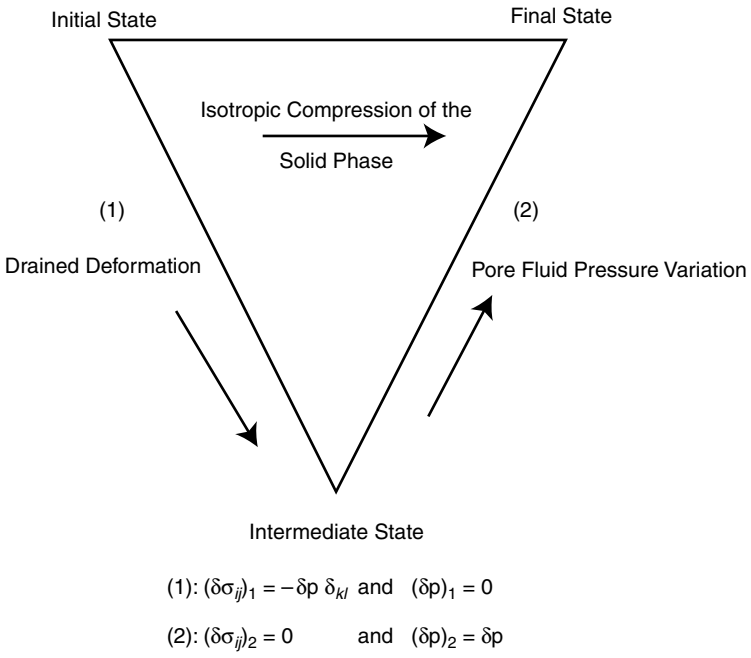

Figure 1.8 ► Isotropic compression of the solid phase in two steps corresponding to: (1) a drained deformation, and (2) a fluid pressure variation at constant external stress.

an incremental deformation $\delta\epsilon_{ij}$ at constant differential stress (Figure 1.8): $\delta\epsilon_{ij} = (S_{ijkl})_s \delta\sigma_{kl}$ in these conditions, with $\delta\sigma_{kl} = -\delta p\ \delta_{kl}$. This incremental deformation can also be written as the superposition of a deformation at constant stress and a deformation at constant pore pressure:

$$\delta\epsilon_{ij} = \left(\frac{\partial\epsilon_{ij}}{\partial p}\right)_{\sigma_{ij}} \delta p + \left(\frac{\partial\epsilon_{ij}}{\partial\sigma_{kl}}\right)_{p} \delta\sigma_{kl} = (\Phi_0\ S'_{ij} - S_{ijkk})\delta p.$$

These relations provide the result

$$S_{ijmm} - (S_{ijnn})_s = \Phi_0\ S'_{ij}. \tag{1.103}$$

Substituting this result into equation (1.102), we arrive at the final relation equivalent to the Biot-Gassmann equation in the anisotropic case:

$$S_{ijkl} - (S_{ijkl})_u = \frac{\left[S_{ijmm} - (S_{ijnn})_s\right]\left[S_{klpp} - (S_{klqq})_s\right]}{\frac{1}{K} - \frac{1}{K_s} + \Phi_0(\frac{1}{K_f} - \frac{1}{K_s})}. \tag{1.104}$$

Equation (1.104) is the Brown-Korringa equation.

1.3 Poroplasticity

Although poroelasticity theory provides a nice and powerful basis to deal with deformations in porous saturated rocks, it is restricted to describing small, reversible strains. Many geological situations correspond to irreversible strains and consequently cannot be handled by poroelasticity theory. Poroplasticity is an extension of plasticity to porous saturated rocks and is an appropriate tool to deal with such situations. The following presentation, however, is restricted to small strains. It can be extended to large strains by introducing a multiplicative decomposition of the plastic and elastic parts.

1.3.1 Fundamental Relations of Poroplasticity

Because an irreversible deformation has to be accounted for, two types of relations are required, as in classical plasticity. The first one is the yield function that defines the conditions for plastic behavior, and the second one concerns the flow and hardening rules that apply during plastic deformation.

Elastic and Plastic Components of Strain and Pore Volume Change

The mechanical loading defined by the stress σ_{ij} and the fluid pressure p induce a strain ϵ_{ij} and an apparent fluid volume fraction change $v - v_0$, which can, in general, be split into a reversible part (elastic), and an irreversible part (plastic). More precisely, it is assumed that it is possible to unload the REV, that is, to return to the initial stress $(\sigma_{ij})_0$ and fluid pressure p_0 through a purely reversible process. As in the section on poroelasticity, both $(\sigma_{ij})_0$ and p_0 are given a value of 0. The REV is then said to be in the unloaded state. With respect to the initial state, the unloaded state is characterized by a strain ϵ_{ij}^p and an apparent fluid volume fraction change $v_p - v_0 = \delta v_p$.

Elastic reloading from the unloaded state restores the stress σ_{ij} and the pore pressure p. It induces the elastic components of strain ϵ_{ij}^e and the apparent pore volume fraction change $\delta v_e = v - v_p$. This can be expressed as

$$\epsilon_{ij} = \epsilon_{ij}^p + \epsilon_{ij}^e \qquad v - v_o = \delta v^e + \delta v^p. \tag{1.105}$$

Let us point out that unloading and reloading between the unloaded state and the final state are reversible processes. This implies that the relationships between σ_{ij}, p, on one hand, and ϵ_{ij}^e, δv^e, on the other, are identical to those derived in the poroelastic case (see previous discussion on linear anisotropic poroelasticity):

$$\sigma_{ij} = C_{ijkl}\,\epsilon_{kl}^e - b_{ij}\,p \qquad \delta v^e = b_{ij}\,\epsilon_{ij}^e + \frac{p}{M}. \tag{1.106}$$

Micromechanical Approach of Poroplastic Behavior

The connection between macroscopic formulations and the micromechanisms of deformations in the case of plastic deformation has been investigated by Rice in a series of papers (Rice, 1971, 1975, 1977). Rice has shown how the microstructural rearrangements within the REV can be related to the macroscopic plastic deformation. In particular, in the case of a porous saturated rock, a specific question is: how do the increments of fluid pore pressure enter constitutive relations? For an elastic response, the section on poroelasticity provides the answer. For a plastic response, the special case of fissured rocks is of great interest. Then, following a similar analysis to that presented for nonlinear poroelasticity, we can decompose any stress state into an isotropic compression of the solid phase, and an additional stress applied to the external rock surface. Assuming a linear elastic behavior for the first stress state, the plastic increment of deformation follows the classical Terzaghi effective stress principle for fissured rocks if we assume that all inelasticity arises by the processes of frictional slippage at solid–solid contacts of isolated asperities or from further stable cracking from crack tips (Rice, 1977).

Yield Function

When is an evolution of the REV of plastic (respectively elastic) nature? The yield function aims at answering that question. The micromechanical point of view provides a guideline for the mathematical formulation of this concept. Let us assume that the solid phase is perfectly elastoplastic. The microscopic yield function is denoted as F_m. It is a function of the six microscopic stresses s_{ij}. The elastic domain in the space of stresses is defined by the condition $F_m(s_{ij}) < 0$. In other words, plastic strains may occur only if the microscopic stress state is on the boundary of the elastic domain defined by $F_m(s_{ij}) < 0$. Positive values of F_m are not physically admissible. More precisely, for an infinitesimal stress increment ds_{ij}, two possibilities exist. Either

$$F_m < 0 \quad \text{or} \quad [F_m = 0 \quad \text{and} \quad dF_m < 0] \Rightarrow \text{elastic evolution} \tag{1.107}$$

or

$$F_m = 0 \quad \text{and} \quad dF_m = 0 \Rightarrow \text{plastic evolution.} \tag{1.108}$$

Let us now consider the REV. If every solid particle inside is strictly experiencing an elastic deformation (i.e., $F_m < 0$), then the REV evolution is elastic. This can be stated mathematically by introducing the following function of the microscopic stress field over the REV:

$$F = \max \; F_m(s_{ij}). \tag{1.109}$$

According to this definition, the condition $F < 0$ implies that every solid particle inside the REV is strictly in the elastic domain. If $F = 0$, there is a region of the solid phase where the microscopic stress state lies on the boundary of the elastic

domain (i.e., $F_m = 0$). The condition $dF < 0$ implies that all the solid's particles return in the elastic domain (i.e., $F_m = 0$ and $dF_m < 0$). If $dF = 0$, the conditions $F_m = 0$ and $dF_m = 0$ may be satisfied in part of the solid phase. In this case, the REV evolution is plastic. The conclusions of the previous discussion can be summarized as follows:

$$F < 0 \quad \text{or} \quad [F = 0 \quad \text{and} \quad dF < 0] \Rightarrow \text{elastic evolution} \tag{1.110}$$

or

$$F = 0 \quad \text{and} \quad dF = 0 \Rightarrow \text{plastic evolution.} \tag{1.111}$$

F is the macroscopic yield function. From its definition, F is a function of the microscopic stress field at the considered time. From a physical point of view, the variation of the residual stress at the microscale that is induced by any plastic process is responsible for the evolution of the elastic domain. This effect is classically referred to as "hardening." A finite set of variables $q^{(1)}, q^{(2)}, \ldots q^{(n)}$ is introduced. The parameters $q^{(i)}$ are referred to as hardening parameters. Their choice should be such that the effect of the residual stress on the macroscopic criterion is described sufficiently well. Eventually, the simplified formulation of the macroscopic yield criterion takes the form

$$F = F(\sigma_{ij}, p, q^{(i)}). \tag{1.112}$$

Flow and Hardening Rules

Using equations (1.110), (1.111), and (1.112), it is possible to determine whether the REV evolution is elastic or plastic. The answer depends on the macroscopic stress and pore pressure σ_{ij}, p, as well as on the hardening parameter q (we assume for simplification that there is only one such parameter). When the initial state is on the boundary of the macroscopic elastic domain ($F = 0$), any infinitesimal increment of the parameters leads to

$$dF = \frac{\partial F}{\partial \sigma_{ij}} d\sigma_{ij} + \frac{\partial F}{\partial p} dp + \frac{\partial F}{\partial q} dq. \tag{1.113}$$

The determination of dq is the purpose of the *hardening rule*. In the case of a plastic evolution, the incremental loading induces an incremental microscopic plastic strain de^p_{ij}, which in turn is responsible for the increment dq. What is the incremental macroscopic strain? We know from equation (1.106) the increments $d\epsilon^e_{ij}$ and dv^e. The plastic increments $d\epsilon^p_{ij}$ and dv^p are given by the *flow rule*. We know that ϵ^p_{ij}, v^p, and q are ultimately functions of e^p_{ij}. The microscopic approach does not specify the hardening and flow rules, but it points to the fact that they

are strongly related. This explains why, at the macroscopic scale, the classical assumption is to choose a similar rule for both flow and hardening:

$$\begin{aligned} d\epsilon_{ij} &= H^{\epsilon}_{ij}\, d\lambda \\ dv^p &= H^v\, d\lambda \\ dq &= H^q d\lambda, \end{aligned} \tag{1.114}$$

where $d\lambda$ is a positive scalar referred to as plastic multiplier:

$$d\lambda > 0 \quad \text{if} \quad F = 0 \quad \text{and} \quad dF = 0 \quad d\lambda = 0 \quad \text{if} \quad F < 0 \quad \text{or} \quad dF < 0. \tag{1.115}$$

The flow and hardening rules are thus prescribed by a new set of functions, H. This set, however, prescribes only the direction of the increment $(d\epsilon^p_{ij}, dv^p, dq)$. The parameter $d\lambda$ is left undetermined. By using equations (1.113) and (1.114) we get

$$dF = \frac{\partial F}{\partial \sigma_{ij}} d\sigma_{ij} + \frac{\partial F}{\partial p} dp + \frac{\partial F}{\partial q} H^q\, d\lambda. \tag{1.116}$$

For any plastic evolution, the condition $[d\lambda > 0$ and $dF = 0]$ implies that

$$d\lambda = \frac{\left(\frac{\partial F}{\partial \sigma_{ij}} d\sigma_{ij} + \frac{\partial F}{\partial p} dp\right)}{-\frac{\partial F}{\partial q} H^q}. \tag{1.117}$$

Defining $\vec{\nabla} F = (\partial F/\partial \sigma_{ij}, \partial F/\partial p)$ and $\vec{\delta L} = (d\sigma_{ij}, dp)$, with $\mathcal{H} = -(\partial F/\partial q) H^q$, we get

$$d\lambda = \frac{1}{\mathcal{H}} (\vec{\nabla} F \cdot \vec{\delta L}). \tag{1.118}$$

This expression is the ratio of a scalar product and a characteristic hardening parameter. The scalar product is between the unit outward normal- oriented to the elastic domain (defined by $F = 0$) and the incremental load.

Let us consider a positive hardening, a situation where $\mathcal{H} > 0$. Then in the case of plastic evolution, $d\lambda > 0$, and from equation (1.118), $\vec{\nabla} F \cdot \vec{\delta L} > 0$. We have also $(\partial F/\partial q) dq < 0$. Because in that case, the hardening effect contributes to a negative increment of dF, as seen from equation (1.116), any plastic process induces an increase of the elastic domain. In contrast, if $\vec{\nabla} F \cdot \vec{\delta L} < 0$, then $dF < 0$, since $\mathcal{H} > 0$ and $d\lambda \geq 0$. Then equation (1.115) yields $d\lambda = 0$. This means that the evolution is elastic. Hence, if the (σ_{ij}, p) state lies on the boundary of the elastic domain $(F = 0)$, the sign of $\vec{\nabla} F \cdot \vec{\delta L}$ controls the nature of the evolution

induced by an incremental loading. These conclusions lead to a new formulation of the hardening and flow rules.

$$\begin{aligned}
(\vec{\nabla} F \cdot \vec{\delta L}) < 0 \Longrightarrow d\epsilon_{ij}^{p} &= 0 \\
dv^{p} &= 0 \\
dq &= 0 \\
(\vec{\nabla} F \cdot \vec{\delta L}) > 0 \Longrightarrow d\epsilon_{ij}^{p} &= H_{ij}^{\epsilon}\, d\lambda. \\
dv^{p} &= H^{v}\, d\lambda \\
dq &= H^{q}\, d\lambda.
\end{aligned} \tag{1.119}$$

In some cases, it may be possible to define a plastic potential g such that $H_{ij}^{\epsilon} = \partial g/\sigma_{ij}$. The flow rule is said to be associated when the vector $(H_{ij}^{\epsilon},\, H^{v})$ is collinear to $\vec{\nabla} F$, which represents the normal to the yield surface $F = 0$ in the $(\sigma_{ij},\, p)$ space. In such a situation, it is possible to set H_{ij}^{ϵ} and H^{v} equal to the derivatives of F with respect to σ_{ij} and p, respectively:

$$H_{ij}^{\epsilon} = \frac{\partial F}{\partial \sigma_{ij}} \qquad H^{v} = \frac{\partial F}{\partial p}. \tag{1.120}$$

This means that $F = g$. The plastic potential is identical to the yield function.

1.3.2 An Example of Hydromechanical Coupling in Poroplasticity: Cam-Clay Model

Initially introduced to model the constitutive behavior of normally consolidated clays, the Cam-Clay model has inspired numerous constitutive models devoted to various soils and rocks. Soils change in volume when plastically sheared, and rocks can also exhibit this type of behavior in crustal conditions. This phenomenon of *dilatancy*, will be examined in detail in other chapters. Let us simply emphasize at this point that it is the main reason for the difference between the drained and undrained deformation regimes of porous rocks and soils. In the drained case, the fluid mass content can change freely, whereas it cannot in the undrained one. If the rock is compacting during a plastic undrained deformation, the pore fluid pressure will rise, whereas the reverse is true for dilating rock. Although the Cam-Clay model is more appropriate for clayey rocks, it will be shown in Chapter 2 that it provides as well a useful framework to analyze the behavior of silicate porous rocks such as sandstones.

General Features

The model is described in terms of the Terzaghi effective pressure $P' = P - p$ and the equivalent deviatoric stress $Q = (3J_2)^{1/2}$, where the second invariant of

the deviatoric stress tensor $J_2 = 1/2(\sigma_{ij}^d \sigma_{ij}^d)$ and $\sigma_{ij}^d = \sigma_{ij} + P\delta_{ij}$. As regards the reversible components of strain, the incremental elastic volumetric strain $d\epsilon_{ii}^e$ in the classical Cam-Clay model is related to the increment of the Terzaghi effective pressure dP' according to a nonlinear state equation of the form

$$d\epsilon_{ii}^e = \frac{dP'}{K(P')}, \tag{1.121}$$

where $K(P') = -k^e P'$. The solid phase is assumed to be plastically incompressible. The yield criterion depends on the effective stress invariants because only the isotropic case is considered. The elastic domain in the (σ_{ij}, p) space can be represented in the P'-Q plane as bounded by an ellipse of equation

$$\begin{aligned} F(\sigma_{ij}, p, P_c) &= G(P', Q, P_c) \\ &= \frac{1}{2}[(P' - P_c/2)^2 + (Q/\mathcal{M})^2 - (P_c/2)^2]. \end{aligned} \tag{1.122}$$

The elastic domain is located in the compressive effective stress field, i.e., $P' > 0$ (Figure 1.9). P_c is usually referred to as the "consolidation pressure" and constitutes the hardening parameter of the Cam-Clay model. It corresponds to the abscissa of the point where the ellipse intersects the P'-axis. The maximum Q_M value on the elliptic boundary is obtained for $P' = P_c/2$, where $Q_M = \mathcal{M}P_c/2$. Indeed, $\mathcal{M}$ being a constant, the P_c value controls the size of the elastic domain. During an isotropic compression, $Q = 0$, so that P_c represents the elastic limit in that case. Then the evolution is elastic up to $P' = P_c$.

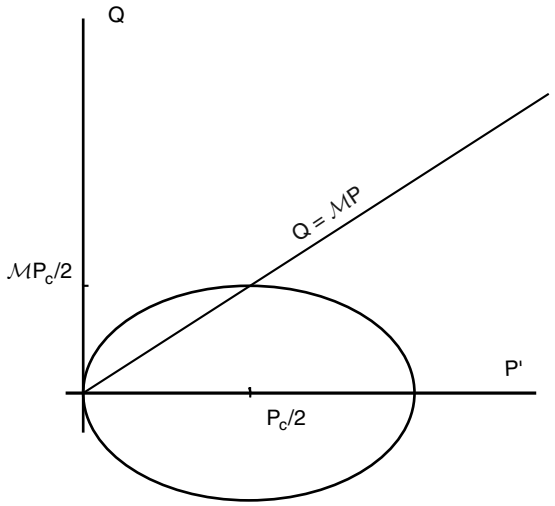

Figure 1.9 ► Cam-Clay model: the ellipse defines the elastic domain in the P'-Q plane.

The flow rule of the Cam-Clay model is associated:

$$d\epsilon_{ij}^p = \frac{\partial F}{\partial \sigma_{ij}} d\lambda \qquad dv^p = \frac{\partial F}{\partial p} d\lambda. \tag{1.123}$$

Moreover,

$$\frac{\partial F}{\partial \sigma_{ij}} = \frac{\partial G}{\partial P'} \frac{\partial P'}{\partial \sigma_{ij}} + \frac{\partial G}{\partial Q} \frac{\partial Q}{\partial \sigma_{ij}} \qquad \frac{\partial F}{\partial p} = -\frac{\partial G}{\partial P'}. \tag{1.124}$$

Combining these last equations, we get

$$\frac{\partial F}{\partial \sigma_{11}} = -\frac{1}{3}(P' - P_c/2) + \frac{3}{2}\frac{\sigma_{11}^d}{\mathcal{M}^2} \tag{1.125}$$

and similar equations by permutation for $\partial F/\partial \sigma_{22}$ and $\partial F/\partial \sigma_{33}$. It follows then that

$$(d\epsilon_{ij}^d)^p = \frac{3}{2\mathcal{M}^2} \sigma_{ij}^d \, d\lambda, \tag{1.126}$$

where $(d\epsilon_{ij}^d)^p$ is the incremental deviatoric plastic strain. The volumetric plastic strain is

$$d\epsilon_{ii}^p = -(P' - P_c/2) \, d\lambda. \tag{1.127}$$

This shows that the plastic domain (the elliptical boundary on Figure 1.9) can be split in two parts. For $P' > P_c/2$, $d\epsilon_{ii}^p < 0$ and there is a volume decrease during plastic deformation, it is a compaction regime. For $P' < P_c/2$, $d\epsilon_{ii}^p > 0$ and there is a volume increase during plastic deformation, it is a dilatancy regime. The limit $P' = P_c/2$ corresponds to the critical state, where there is no volume variation.

To model the hardening phenomenon, we have to define how the hardening parameter $q = P_c$ is modified by a given plastic evolution. Experimental data suggest relating the consolidation pressure P_c to the plastic volumic ϵ_{ii}^p by an exponential law:

$$P_c = P_c^0 \, \exp(-k^p \epsilon_{ii}^p) \quad \text{for} \quad P_c > P_c^0, \tag{1.128}$$

where P_c^0 is the initial elastic limit under isotropic compression. Combining equations (1.121), (1.127), and (1.128) for the case of an isotropic compression yields

$$d\epsilon_{ii} = -\frac{1}{k} \frac{dP'}{P'}, \tag{1.129}$$

where $1/k = 1/k^e + 1/k^p$, because in that case $P_c = P'$. Thus the plot of the total volumetric strain ϵ_{ii} versus $\log P'$ is a straight line with a slope $-1/k$. Let us point out that k^e represents the slope of an elastic unloading path in the ϵ_{ii}-$logP'$ plane.

A very important assumption of the Cam-Clay model is that equation (1.128) remains valid under nonisotropic loadings. This implies that the effect of the

deviatoric plastic strain on the hardening phenomenon is believed to be negligible. In other words, it is assumed that hardening is controlled by plastic densification. We can now reformulate the hardening rule as follows:

$$\begin{aligned} dP_c &= -k^p P_c \, d\epsilon_{ii}^p \\ &= -k^p P_c tr \frac{\partial F}{\partial \sigma_{ij}} d\lambda \quad \Rightarrow \quad H^q = H^{P_c} = -k^p P_c tr \frac{\partial F}{\partial \sigma_{ij}}. \end{aligned} \tag{1.130}$$

Finally, the hardening modulus $\mathcal{H}$ is determined from equation (1.130) together with equation (1.125):

$$\mathcal{H} = \frac{k^p}{2} P' P_c \left(P' - \frac{P_c}{2} \right). \tag{1.131}$$

Recalling that $P' > 0$, the positive hardening condition $\mathcal{H} > 0$ requires that $P' > P_c/2$. This corresponds to effective stress states located on the right side of the ellipse. In this domain, equation (1.127) indicates as previously discussed a strictly compacting plastic behavior, $d\epsilon_{ii}^p < 0$, associated with a positive hardening, $dP_c > 0$. In contrast, if $P' = P_c/2$, that is, if the stress state is located at the intersection between the straight line $Q = \mathcal{M} P'$ and the ellipse, the tensor $\partial F/\partial \sigma_{ij}$ is purely deviatoric so that the hardening modulus $\mathcal{H} = 0$. We can expect that this critical stress state corresponds to a localization of the deformation, as discussed in Chapter 5. This statement can be illustrated with a particular experiment: consider an isotropic stress state such as $P' = P_c^0$, $Q = 0$, and let the deviatoric stress Q steadily increase while P' is kept constant. From equations (1.118) and (1.131), using (1.127), it follows that

$$d\epsilon_{ii}^p = -\frac{2Q dQ}{k^p P' P_c \mathcal{M}^2}. \tag{1.132}$$

Equation (1.132) can be integrated by using equation (1.128), to find

$$P_c = P_c^0 + \frac{Q^2}{\mathcal{M}^2 P'}. \tag{1.133}$$

Equation (1.133) describes the positive hardening induced by the deviatoric loading. The hardening is the consequence of the compaction, and the plastic volumetric strain is

$$\epsilon_{ii}^p = -\frac{1}{k^p} \log(1 + \frac{\zeta^2}{\mathcal{M}^2}), \tag{1.134}$$

where $\zeta = \frac{Q}{P'}$. Let us introduce the scalar increment of deviatoric strain defined as

$$(d\varepsilon^d)^p = \left[(d\epsilon_{ij}^d)^p (d\epsilon_{ij}^d)^p \right]^{1/2}. \tag{1.135}$$

From equation (1.126), we obtain

$$(d\varepsilon^d)^p = \frac{2\sqrt{6}}{k^p \mathcal{M}^4} \frac{\zeta^2 d\zeta}{1 - (\frac{\zeta}{\mathcal{M}})^4}. \tag{1.136}$$

Then, by integration,

$$(\varepsilon^d)^p = \frac{\sqrt{3/2}}{k^p} \left[\frac{\mathcal{M} + \zeta}{\mathcal{M} - \zeta} - 2 \arctan \frac{\zeta}{\mathcal{M}} \right]. \tag{1.137}$$

This last expression confirms that large plastic deviatoric strains develop when the stress ratio ζ becomes close to $\mathcal{M}$, i.e., when the stress state is close to the intersection between the ellipse and the straight line $Q = \mathcal{M} P'$. Note that the deviatoric strain becomes infinite whereas the volumetric strain remains finite. The straight line $Q = \mathcal{M} P'$ is often referred to as the critical-state line.

The Undrained Shear Test

For simplicity, let us assume that the fluid phase is incompressible. Let us assume also that the solid phase is both elastically and plastically incompressible. With these simplifications, any undrained test corresponds to a total macroscopic volumetric strain equal to 0. Let the equivalent shear stress Q increase, while keeping constant the total mean stress P. In the initial state, the stress state is purely isotropic, $Q = 0$, and is located on the yield surface, $P'_0 = P'^0_c$. As previously, we investigate the domain of positive hardening. In that domain, we know that any plastic evolution is a compaction. Consequently, a dilatant elastic volumic strain must balance the plastic strain:

$$d\epsilon^e_{ii} = -\frac{1}{k^e} \frac{dP'}{P'} = -d\epsilon^p_{ii} \geq 0. \tag{1.138}$$

Thus, the compacting plastic behavior induces a decrease of the effective stress $P' = P - p$. Because P is kept constant, this means that the loading induces an increase of pore pressure p. More precisely, equations (1.128) and (1.138) lead to

$$\frac{dP_c}{P_c} = -\frac{k^p}{k^e} \frac{dP'}{P'} \Rightarrow \frac{P_c}{P^0_c} = \left(\frac{P'}{P'_0} \right)^{-k^p/k^e}. \tag{1.139}$$

Equation (1.139) indicates that hardening ($dP_c > 0$) is associated with a decrease of P'. Using as before $\zeta = Q/P'$, equation (1.122) provides the equation of the effective stress path in the P'-Q plane:

$$\frac{P'}{P'_0} = \frac{1}{\left(1 + \frac{\zeta^2}{\mathcal{M}^2}\right)^{\Lambda}}, \tag{1.140}$$

where $\Lambda = [1 + (k^p/k^e)]^{-1}$. Again we can note that the increase of shear stress Q induces a decrease of the effective pressure P', and thus an increase of pore pressure p. The maximum value of $\zeta = Q/P'$ is equal to $\mathcal{M}$, for which $P' = P_c/2$ and $\mathcal{H} = 0$. As in the drained shear test, this state can be interpreted as a failure through large deviatoric strains. The corresponding failure shear stress Q^f_{und} is usually referred to as the undrained shear strength and can be readily derived from equation (1.140):

$$Q^f_{und} = \mathcal{M}\frac{P'_0}{2^\Lambda}. \tag{1.141}$$

This result shows that the undrained shear strength depends linearly on the consolidation pressure $P^0_c = P'_0$.

1.4 Rupture

In the low-pressure and low-temperature conditions of the upper crust, rock failure occurs when stresses are increased above a certain limit. Poroplastic models in general do not account for this type of behavior. On the other hand, poroelasticity is appropriate for analyzing small reversible deformations, but irreversible deformations have to be analyzed either through phenomenological constitutive laws (for example, poroplasticity) or rupture theory. Models described in previous sections are rooted in classical continuum mechanics, although this is an idealized view because porous rocks are made of minerals and pores (very flat pores are called cracks). Rock failure corresponds to the development of a major discontinuity. At small scales, such discontinuities exist: these are cracks. Rock failure is in general the result of crack propagation. When crack size is comparable to grain size or lower, it is usually described as a microcrack. We do not examine here the various possible origins of microcracks, because we are interested only in the consequences of their presence. Cracks of different sizes can be observed on rock samples in the laboratory or outcrops in the field. From microcracks to macroscopic fractures, joints, and fault zones, a broad range of scales exists (Scholz, 1990; Davy, 1993; Main, 1996). Rock failure can also be addressed from the point of view of bifurcation theory. This will be presented extensively in Chapter 5. Bifurcation theory accounts for the existence of a strain discontinuity. Such an approach is very relevant to deal with strain localization.

1.4.1 Linear Fracture Mechanics

For many years, the concept of a characteristic stress beyond which any brittle solid fails has been used by engineers. Although this is an attractive model, it became suspect when it was realized that it could not explain the failures of large structures such as ships or planes. The identification of the fracture mechanisms

and the development of a sound theory based on first principles resulted from Griffith's ideas and experiments.

Stress Concentration and Energy Balance

Although most of the situations we are interested in correspond to compressive stresses, we first examine the response of rocks to tensile stresses. It is well known that rocks, as do other brittle solids, exhibit a tensile strength that is much lower than their compressive strength. The breakthrough in understanding tensile strength of solids is owed to Griffith (1920). The starting point is to recognize that cracks are the elementary defects responsible for failure in brittle solids. Assuming the solid to be elastic, Griffith's model contains two basic ideas that have proved to be very fruitful.

The first one points to the importance of stress concentrations induced by crack tips in an elastic medium (Figure 1.10). A simple, well-known, and important example of stress concentration in geophysics is that concerning a cylindrical borehole. In that case, the stress amplification (ratio of local tensile stress at the borehole boundary relative to tensile stress at great distance σ) factor is only 3. In the case of an elliptical crack, the amplification factor is $(1 + 2\sqrt{c/r})$, where

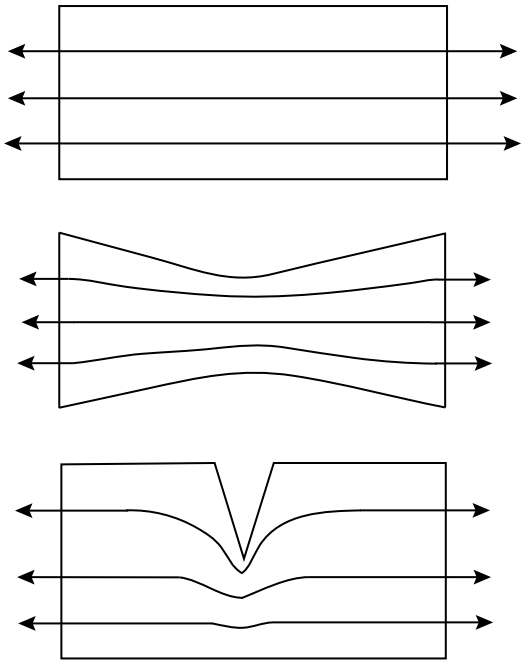

Figure 1.10 ► Stresses trajectories around a crack tip.

c is the crack radius and r the radius of curvature at the crack tip. Obviously, if r approaches atomic spacing values and c is on the order of 10 μm to 1 mm, the amplification factor gets very high. This provides a nice mechanism to explain why cracks are potentially dangerous and can propagate even if the far-field tensile stress is moderate.

Crack propagation requires some energy. Griffith's second idea explains where this energy comes from. This is the energy-balance concept (Lawn, 1993): the rock containing a crack and the loading device are considered as a single reversible thermodynamic system. Following Engelder (1993), this system can be represented schematically as done in Figure 1.11. The total energy of the system is the addition of a mechanical energy and a surface energy. This last term results simply from the existence of two surfaces, which are the crack faces. Creating two crack faces of area S in an intact solid corresponds to a cost in energy of $2\gamma S$, where γ is the thermodynamic surface energy per unit area. For the situation described in Figure 1.11, and with $2c$ as the crack length, the surface energy per unit length of fracture front can be written as

$$U_S = 4c\gamma. \tag{1.142}$$

The total energy of the system is the sum of U_S and a mechanical energy U_M, which is given by

$$U_M = U_E - W, \tag{1.143}$$

where U_E is the elastic potential energy stored in the rock and $-W$ is the potential energy of the loading device, expressed as the negative of the work associated with any displacement of the loading points. Because the applied load is constant, we can use the general result $W = 2U_E$, so that the total mechanical energy is

$$U_M = -U_E. \tag{1.144}$$

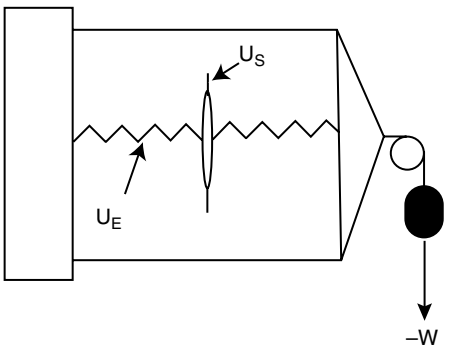

Figure 1.11 ► Reversible thermodynamic system relative to the Griffith energy balance concept: rock containing a crack and the loading device.

In the present case, the elastic energy for an elliptical crack is, per unit of crack front (Lawn, 1993),

$$U_E = \pi \frac{(1-\nu^2)}{E} \sigma^2 c^2, \tag{1.145}$$

where ν is the rock's Poisson ratio, E is the Young modulus, and σ the far-field tensile stress. Although we do not derive here the exact result given previously, a simple way to understand it is to consider a rock sample submitted to a tensile stress σ. In the case of an intact rock, the elastic energy per unit volume would be $\sigma^2/2E$. For a cracked rock, and for a unit length perpendicular to the plane of Figure 1.11, the area where the crack strongly affects the stress field is on the order of πc^2. This implies that $U_E \sim \pi c^2(\sigma^2/2E)$. If we consider a virtual crack extension dc, the mechanical energy will decrease as the crack extends. This provides the driving force for crack propagation. However, the surface-energy term will increase and this will oppose crack propagation. The basic idea Griffith had was to look for the minimum energy situation:

$$\frac{dU}{dc} = 4\gamma - 2\pi \frac{(1-\nu^2)^2}{E} c = 0. \tag{1.146}$$

According to Griffith's theory, a crack would extend or retract reversibly, depending on the sign of dU/dc.

The above result can be expressed in terms of stress. Let us call σ_c the critical stress for which a crack of length $2c$ becomes unstable. Then

$$\sigma_c = \sqrt{\frac{2\gamma E}{\pi c(1-\nu^2)}}. \tag{1.147}$$

For instance, if $c = 1$ mm, $E = 10^{11}$ Pa, $\nu = 0.25$, and $\gamma = 1$ J·m^2, we get $\sigma_c = 8$ MPa. The largest cracks are the most dangerous ones. Griffith's result shows clearly why the idea of a critical stress, viewed as a material property, is wrong. The σ_c value depends not only on material properties such as E and ν, but also on microstructural parameters such as c.

Fracture Propagation Modes

Generalizing Griffith's approach, linear elastic fracture mechanics provides a general basis to analyze crack stability in various cases. From a geometrical point of view, there are three basic fracture propagation modes. The previous situation corresponds to mode I (Figure 1.12). In that case, it can be shown (Sih and Liebowitz, 1968) that, for a stationary crack, the form of solution is

$$\sigma_{ij} = \frac{K_I}{\sqrt{r}} f_{ij}(\theta) + T\delta_{i1}\delta_{j1} + A_{ij}(\theta)\sqrt{r} + B_{ij}(\theta)r + ... \tag{1.148}$$

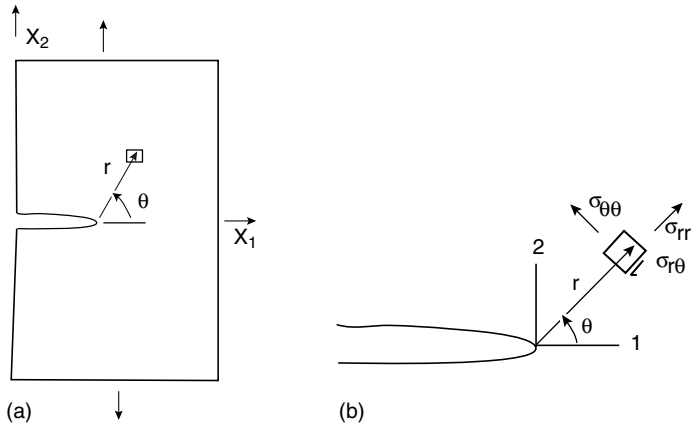

Figure 1.12 ► Mode I. The boundary conditions are such that in the far field $\sigma_{22} = \sigma_\infty$, and at the crack boundaries $\sigma_{2j} = 0$. (a) The polar coordinates of any point near the crack tip are (r, θ). In polar coordinates, the stresses are $\sigma_{rr}, \sigma_{\theta\theta}, \sigma_{r\theta}$ (b).

K_I is called the "stress intensity factor," and $f_{ij}(\theta)$ is normalized so that the parameter $f_{22(0)=1/\sqrt{2\pi}}$. The two-dimensional solution can be compared with that of Griffith (1920), and this leads to the result

$$K_I = \sigma_\infty \sqrt{\pi c}. \tag{1.149}$$

Near the crack tip, the stress becomes very large: $\sigma_{22}(\theta = 0) = K_I/\sqrt{2\pi r} + ...$ The displacement discontinuity is

$$\triangle u_2 = u_2\,|_{\theta=\pi} \;-\; u_2\,|_{\theta=-\pi} \;=\; \frac{4(1-\nu)}{\mu} K_I \sqrt{r'/2\pi}. \tag{1.150}$$

The three modes of crack tip response are presented in Figure 1.13. For $\theta = 0$, close to the crack tip, the relevant stresses for each mode can be written as

$$\begin{aligned} \sigma_{22} &= \frac{K_I}{\sqrt{2\pi r}} \\ \sigma_{21} &= \frac{K_{II}}{\sqrt{2\pi r}} \\ \sigma_{23} &= \frac{K_{III}}{\sqrt{2\pi r}}. \end{aligned} \tag{1.151}$$

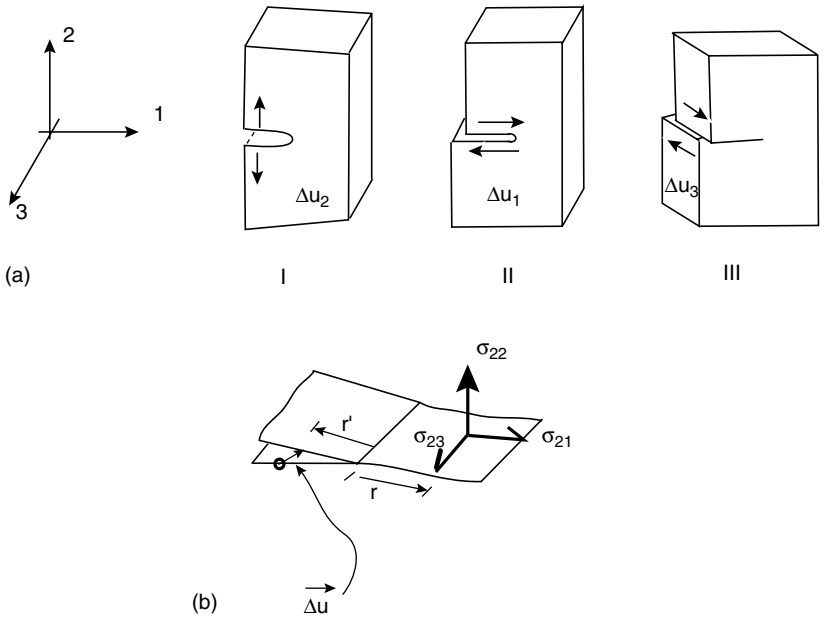

Figure 1.13 ► (a) The three fracture propagation modes. I, tensile; II, in-plane shear; III, antiplane shear. (b) Dominant stress (on prolongation of crack plane) and crack displacement discontinuity for the three modes. Mode I: σ_{22}, Δu_2; Mode II: σ_{21}, Δu_1; Mode III: σ_{23}, Δu_3.

The three displacement discontinuities are

$$\begin{aligned} \triangle u_2 &= \frac{4(1-\nu)}{\mu}\sqrt{\frac{r'}{2\pi}}K_I \\ \triangle u_1 &= \frac{4(1-\nu)}{\mu}\sqrt{\frac{r'}{2\pi}}K_{II} \\ \triangle u_3 &= \frac{4(1-\nu)}{\mu}\sqrt{\frac{r'}{2\pi}}\frac{K_{III}}{(1-\nu)}. \end{aligned} \tag{1.152}$$

The detailed solutions can be found in Lawn (1993). Let us note that the K factors depend on only the outerboundary conditions, i.e., on the applied loading and sample geometry. The stress field exhibits a singularity at the crack tip. This means that one should not use the previous solutions at very small r values. Obviously, the near-field solution should not be used either at large r values because higher-order terms have to be taken into account in that case.

Because the solid is linear elastic, the principle of superposition applies, and for a mixed mode, K terms from superposed loadings are additive.

Mechanical Energy Release Rate

We assume as previously that a crack is present in a linear elastic rock. If $\mathcal{P}$ is the force (per unit thickness) applied to the rock and $\mathcal{U}$ the work-conjugate displacement (Figure 1.14), then for a constant c, $\mathcal{P}d\mathcal{U} = dU_E$, where U_E is the elastic strain energy for a unit thickness. If c is not constant, the elementary variation of elastic strain energy is

$$dU_E = \mathcal{P}d\mathcal{U} - \mathcal{G}dc, \tag{1.153}$$

From the previous relation, we can define the mechanical energy release rate (per unit crack area) $\mathcal{G}$ as

$$\mathcal{G} = -\left(\frac{\partial U_E}{\partial c}\right)_{\mathcal{U}} = -\left(\frac{\partial (U_E - \mathcal{P}\mathcal{U})}{\partial c}\right)_{\mathcal{P}}. \tag{1.154}$$

To find $\mathcal{G}$, let us consider a crack propagation by an increment δ as shown in Figure 1.14 for mode I. Before propagation, the crack tip is located at A. There exists a stress field ahead of A, which is known from fracture mechanics. For instance, at point M, $\sigma_{22} = \sigma_{22}(\delta - \beta, 0)$ since at M, $r = \delta - \beta$ and $\theta = 0$. But the displacement

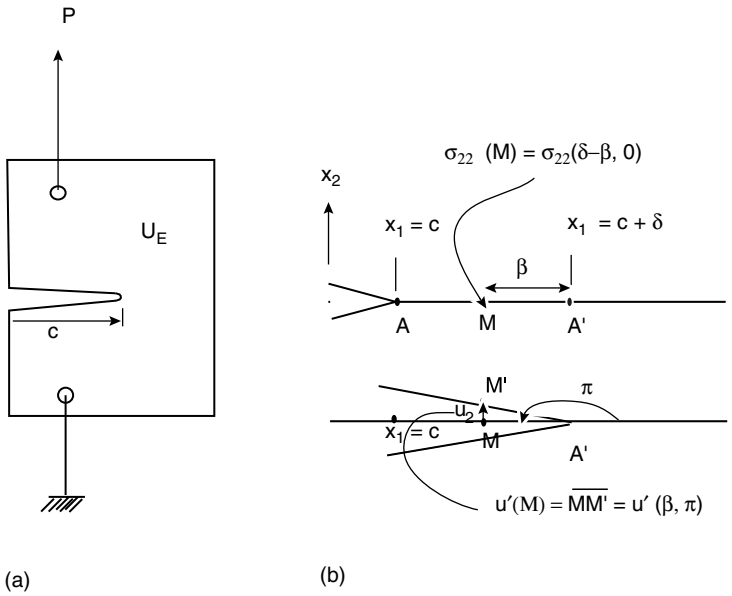

Figure 1.14 ► (a) A half crack in an elastic rock submitted to a tensile force per unit thickness $\mathcal{P}$. (b) Propagation of a crack (mode I) in its plane. The crack propagates from A to A′. When the crack tip is at A, the tensile stress at M is $\sigma_{22} = \sigma_{22}(\delta - \beta, 0)$. When the crack tip is at M′, $\sigma'_{22} = 0$, and $MM' = u' = u'(\beta, \pi)$.

$u_2 = 0$ at M. After propagation from A to A′, the stress σ'_{22} is relaxed on the crack boundary so that at M', $\sigma'_{22} = 0$, and $u'_2 = u'_2(\beta,\ \pi)$. Because the behavior is that of a linear elastic body, the released elastic energy for a propagation δ is $\Delta U_E = -\mathcal{G}_I\delta = 2\int_0^\delta 1/2\ (sigma_{22}u'_2\ d\beta)$. Since both σ_{22} and u'_2 are known, the mechanical energy release is derived from the preceding relation:

$$\mathcal{G}_I = \frac{K_I^2}{E} \tag{1.155}$$

for plane stress conditions. Similar results are obtained for modes II and III:

$$\mathcal{G}_{II} = \frac{K_{II}^2}{E} \qquad \mathcal{G}_{III} = \frac{K_{III}^2(1+\nu)}{E}. \tag{1.156}$$

Let us point out that $\mathcal{G}$ terms from superposed loadings in different modes are additive.

Griffith's result can be obtained from the equilibrium condition

$$\mathcal{P}d\mathcal{U} = dU_E + 2\gamma dc. \tag{1.157}$$

From equation (1.153), this implies

$$\mathcal{G} = \mathcal{G}_c = 2\gamma. \tag{1.158}$$

This allows extension of Griffith's result into a more general analysis of stability. In any mode, cracks are stable up to the limit given by the previous relation. Because there is a direct link between K and $\mathcal{G}$ values, it is possible to write the stability criteria in terms of either $K = K_c$ or $\mathcal{G} = \mathcal{G}_c$.

Crack Paths

Although fracture mechanics appears to be a powerful tool to deal with crack stability conditions, there is an additional complexity that we have not mentioned. The preceding criteria give us the conditions at which cracks become unstable and therefore start to propagate. They do not provide, however, any indication about the direction in which they will propagate. Assuming that any crack propagates in its original plane is a simple, but wrong, assumption. The reason for that is related to the symmetry of the crack tip stress field. Obviously, only mode I produces a symmetric stress field (with respect to the axis Ox_2 in Figure 1.14). It follows that, in mode I, the tensile stress $\sigma_{\theta\theta}$ at the crack tip is maximum in the plane $x_2 = 0$. In that case, and only in that case, the crack propagates in its own plane. For modes II and III, the lack of symmetry with respect to the plane $x_2 = 0$ implies that the tensile stress $\sigma_{\theta\theta}$ at the crack tip is not maximum in that plane. As a consequence, crack propagation takes place in a new plane, rotated with respect to the initial plane. The crack looks for the plane of maximum tensile stress. For a more complete analysis, the reader is referred to Lawn (1993).

1.4.2 Failure Criteria for Porous Rocks

In the earth's crust, there is always a component of compressive stress field. For that reason, the linear elastic fracture mechanics framework is not sufficient to deal with failure of porous rocks in situ. Indeed, Griffith's analysis provides a nice way to understand the *initiation* of crack and fracture propagation in silicate rocks. Unless the rock is submitted to pure mode I, however, the results of the previous section imply that any crack is likely to stop after some propagation. This is because, in a mixed mode, any crack leaves its original plane, turns into a *wing* crack, and then becomes stable again.

Micromechanical Approach

On a small scale, the failure of a silicate rock sample submitted to a partly compressive stress field is the result of microcracks propagation and coalescence. Paterson (1978) has summarized the various physical models that have been used. Some physical insight into the behavior of a population of stressed cracks can be obtained by looking at crack–crack interactions as suggested by Kachanov (1993).

Let us consider a single, traction-free crack in an isotropic, linear elastic solid, uniformly loaded on its boundary. This situation is equivalent to that of the same solid with traction applied to the crack faces and a free solid boundary, with a difference that is a homogeneous stress state. Indeed, the second situation (traction applied to the crack faces, solid boundary free) can be obtained by adding to the first one (traction-free crack, solid boundary loaded) an appropriate and identical load on both the external solid boundary and the internal crack face (Figure 1.15). The homogeneous stress state corresponding to this last situation would exist if no crack was present.

We will concentrate in the following on situations where crack faces are loaded. The stress and displacement fields generated by a loaded crack in a linear elastic solid can be represented by a superposition of the fields produced by modes I, II, and III. The solutions are summarized by Kachanov (1993), who pointed to an interesting feature of the mode I field in the two-dimensional case

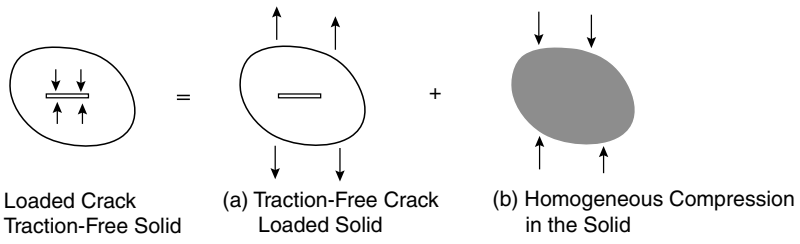

Figure 1.15 ► Loaded crack in an unloaded solid. This situation is equivalent to the superimposition of (a) an unloaded crack in a loaded solid, (b) an identical load applied on both the external surface and the internal crack faces (as if there was no crack).

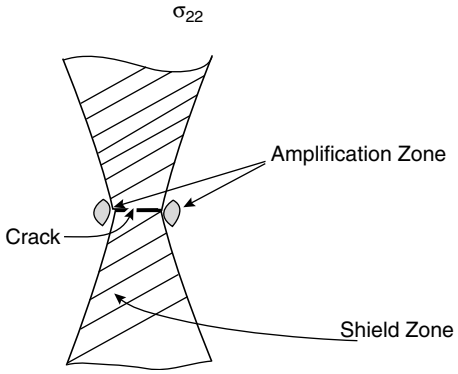

Figure 1.16 ► Stress field σ_{22} in the case of mode I. Note the existence of a shield zone above and below the crack and that of an amplification zone at the crack tips.

(Figure 1.16): there exists in that case a region of compressive stress that is rather large above and below the crack, whereas a small tensile region is present at the crack tips. This has important consequences for crack interactions when a population of cracks is considered. If a second crack is placed approximatively above a first one, there will be a shielding effect. If it is lined up with the first one, an amplification effect is expected. Since all rocks contain many cracks, such interactions have to be accounted for.

An interesting series of experiments was conducted by Hallam and Ashby (1990), which simulated with sheets of poly-methyl-methacrylate the development of wing cracks and their interactions. Figure 1.17 shows two situations that differ by the initial crack's relative position. These pictures show clearly that, when crack centers are in positions such that their interaction is amplified, coalescence of cracks leads to a macroscopic fracture. Kachanov (1982) has shown that wing crack propagation, together with crack roughness, can account for the dilatancy obs/erved before failure.

Macroscopic Criteria of Failure

Schematically, the mechanical behavior of a porous rock beyond its elastic limit, in a compressive stress field, can be analyzed as a two-step process. The first one corresponds to the limited crack propagation described in the previous section. This process will be investigated further in Chapter 4. The second one is macroscopic failure. As a result of macroscopic brittle failure, the rock loses its mechanical strength, and a macroscopic discontinuity develops. Because $K_{I,II,III} = K^c_{I,II,III}$ or $\mathcal{G}_{I,II,III} = \mathcal{G}^c_{I,II,III}$ is valid only for determining the onset of individual crack propagation, linear elastic fracture mechanics does not provide any macroscopic failure criteria (except in mode I). Indeed, the preceding analysis applies to both porous and nonporous rocks. Brittle failure is attained at a peak of deviatoric stress

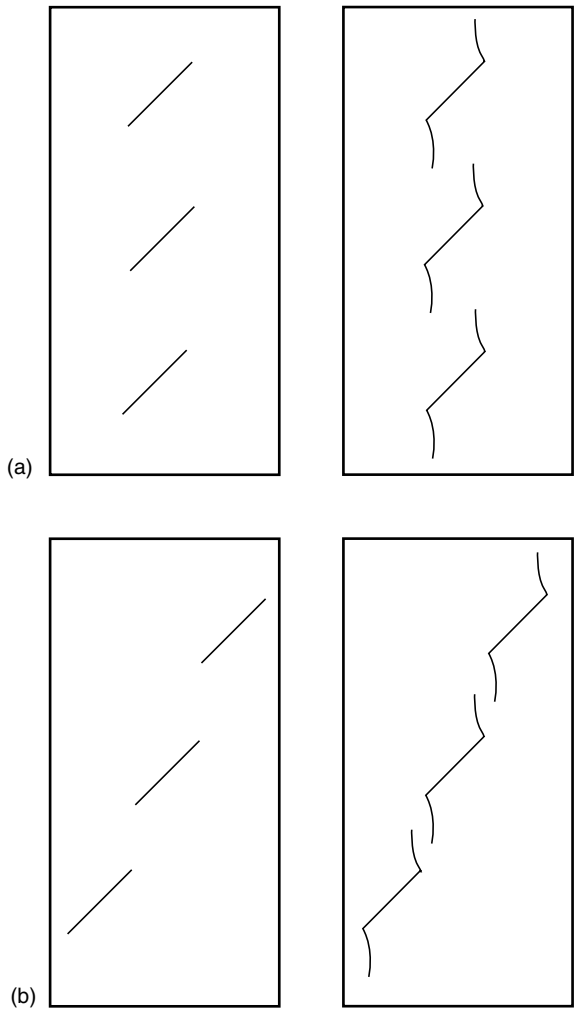

Figure 1.17 ► (a) A sequence of wing crack propagation and crack interactions, under progressively higher compressive stresses (mixed mode). Note that the crack centers are located in the shield zone defined in Figure 1.16. Cracks do not coalesce. (From Hallam and Ashby, 1990). (b) A similar sequence in the case where the crack centers are located in the amplification zone defined in Figure 1.16. Cracks coalesce, and a macroscopic fracture is formed, which contains a coarse gouge. (From Hallam and Ashby, 1990).

at small strains. The peak stress increases with confining pressure, and the post-peak deformation exhibits strain softening. Difference between porous and non-porous rocks are observed when considering the brittle–plastic transition (Wong et al., 1997). Cataclastic flow is an intermediate step in the brittle plastic transition.

In low-porosity rocks, dilatancy takes place and the yield stress shows a positive pressure dependence. In moderate- to high-porosity rocks, compaction takes place and the yield stress decreases with increasing effective pressure. Chapter 2 examines this complex behavior for compaction; Chapter 5 describes and analyzes the localization process.

Bibliography

Batzle, M., Hoffman, R., Han, D.H., and Castagna, J. Fluids and frequency dependent seismic velocity of rocks. *The Leading Edge* 20: 168–171, 2001.

Biot, M.A. General theory of three-dimensional consolidation. *Journal of Applied Physics* 12, 155–164: 1941.

Biot, M.A. Theory of elasticity and consolidation for a porous anisotropic solid. *Journal of Applied Physics* 26: 182–185, 1955.

Biot, M.A. General solutions of the equations of elasticity and consolidation for a porous material. *Journal of Applied Mechanics* 78: 91–96, 1956.

Biot, M.A. Theory of finite deformation of porous solids. *Indiana University Mathematics Journal* 21: 597–620, 1972.

Biot, M.A. Non linear and semi-linear rheology of porous solids. *Journal of Geophysical Research* 78: 4924–4937, 1973.

Biot, M.A., and Willis, D.G. The elastic coefficients of the theory of consolidation. *Journal of Applied Mechanics* 24: 594–601, 1957.

Boutéca, M.J., Kessler, N., Boisson, M., Fourmaintraux, D., and Bary, D. Contribution of poroelasticity to reservoir engineering: lab experiments, application to core decompression and implication in HP-HT reservoirs depletion, paper SPE/ISRM 28093, *Eurock 94, Rock Mechanics in Petroleum Engineering*, pp. 525–533, Balkema, Rotterdam, 1994.

Brown, R.J.S., and Korringa, J. On the dependence of the elastic properties of porous rock on the compressibility of the pore fluid. *Geophysics* 40: 608–616, 1974.

Carroll, M.M. An effective stress law for anisotropic elastic deformation. *Journal of Geophysical Research* 84: 7510–7512, 1979.

Coussy, O. Mécanique des Milieux Poreux, *Technip,* Paris, 1991.

Davy, P. On the fault frequency-length distribution of the San Andreas fault. *Journal of Geophysical Research* 98: 12141–12151, 1993.

De Buhan, P., Chateau, X, and Dormieux, L. The constitutive equations of finite strain poroelasticity in the light of a micro-macro approach. *European Journal of Mechanics, A/Solids* 17: 909–921, 1998.

Detournay, E., and Cheng, A.H.D. Fundamentals of poroelasticity. In *Comprehensive Rock Engineering*, Hudson, J.A., ed., vol.2, pp. 113–171, Pergamon Press, Oxford, 1993.

Deudé, V., Dormieux, L., Kondo, D., and Maghous, S. Micromechanical approach to non linear poroelasticity—Application to cracked rocks, *Journal of Engineering Mechanics,* vol. 128, 2002.

Dormieux, L., Molinari, A., and Kondo, D. Micromechanical approach to the behavior of poroelastic materials. *Journal of the Mechanics and Physics of Solids,* 2002.

Dvorkin, J., Nolen-Hoeksema, R., and Nur, A. Squirt-flow mechanism: Macroscopic description. *Geophysics* 59, 428–438, 1994.

Engelder, Y. *Stress Regimes in the Lithosphere,* p.457, Princeton University Press, 1993.

Guéguen, Y., and Palciauskas, V.V. *Introduction to the Physics of Rocks,* p.294, Princeton University Press, 1994.

Griffith, A.A. The phenomena of rupture and flow in solids. *Philosophical Transaction Royal Society London* A221: 163, 1920.

Hallam, S.D., and Ashby, M.F. Compressive brittle failure and the construction of multi-axial failure maps. In *Deformation processes in Minerals, Ceramics, and Rocks,* Barber, D.J., and Meredith, P.G., eds., pp. 84–108, Unwin Hyman, London, 1990.

Kachanov, M. A microcrack model of rock inelasticity, part II: Propagation of microcracks. *Mechanics of Materials* 1: 29–41, 1982.

Kachanov, M. Elastic solids with many cracks and related problems. *Advances in Applied Mechanics* 30: 259–445, 1993.

Lawn, B. *Fracture of Brittle Solids,* p.378, Cambridge University Press, 1993.

Le Ravalec, M., and Guéguen, Y. Permeability models heated saturated igneous rocks. *Journal of Geophysical Research* 99: 24251–24261, 1994.

Le Ravalec, M., and Guéguen, Y. High and low frequency elastic moduli for saturated porous/cracked rock—differential self-consistent and poroelastic theories. *Geophysics* 61: 1080–1094, 1996.

Lehner, F.K. A review of linear poroelasticity. Unpublished report, Rijswijk, 1997.

McTigue, D.F. Thermoelastic response of fluid saturated porous rock. *Journal of Geophysical Research* 91: 9533–9542, 1986.

Main, I. Statistical physics, seismogenesis, and seismic hazard. *Reviews of Geophysics* 34: 433–462, 1996.

Palciauskas, V.V., and Domenico, P.A. Characterisation of drained and undrained response of thermally loaded repository rocks. *Water Resources Research* 18: 281–290, 1982.

Paterson, M.S. *Experimental Rock Deformation. The Brittle Field,* p.254, Springer, New York, 1978.

Rice, J.R. Inelastic constitutive relations for solids: an internal variable theory and its application to metal plasticity. *Journal of Mechanics and Physics of Solids* 19: 433–455, 1971.

Rice, J.R. Continuum mechanics and thermodynamics of plasticity in relation to microscale deformation mechanisms. In *Constitutive Equations in Plasticity,* Argon, A.S., ed., pp. 23–79, M.I.T. Press, 1975.

Rice, J.R., and Cleary, M.P. Some basic stress diffusion solutions for fluid-saturated elastic porous media with compressible constituents. *Review of Geophysics* 14: 227–241, 1976.

Rice, J.R. Pore pressure effects in inelastic constitutive formulations for fissured rock masses. In *Advances in Civil Engineering through Engineering Mechanics,* pp. 360–363, ASCE, New York, 1977.

Rudnicki, J.W. Coupled deformation-diffusion effects in the mechanics of faulting and failure of geomaterials, *Applied Mechanics Review,* 2002.

Scholz, C.H. *The Mechanics of Earthquakes and Faulting,* p. 439, Cambridge University Press, 1990.

Sih, G.C., and Liebowitz, H. Mathematical theories of brittle fractures, vol. 2. In *Fracture: An Advanced Treatise,* Liebowitz, H., ed., pp. 67–190, Academic Press, 1968.

Thompson, M., and Willis, J.R. A reformulation of the equations of anisotropic poroelasticity. *Journal of Applied Mechanics* 58: 612–616, 1991.

von Terzaghi, K., and Frölich, O.K. *Theorie der Setzung von Tonschichten,* Franz Deuticke, Leipzig, Wien, 1936.

Wang, H. *Theory of Linear Poroelasticity with Applications to Geomechanics and Hydrogeology,* p. 287, Princeton University Press, Princeton, 2000.

Wong, T.F., David, C., and Zhu, W. The transition from brittle faulting to cataclastic flow in porous sandstones: Mechanical deformation. *Journal of Geophysical Research* 102: 3009–3025, 1997.

Zimmerman, R.W. *Compressibility of Sandstones,* p.173, Elsevier, Amsterdam, 1991.

Zimmerman, R.W. Micromechanics of poroelastic rocks. In *Heterogeneous Media,* Markov, K., and Preziosi, L., eds, Birkhauser, Boston, 2000.